Technische Universität München
Fakultät für Medizin

TUM

A mouse model of partial hepatectomy for studying the effect of the gut microbiota on liver regeneration

Yuhan Yin

Vollständiger Abdruck der von der Fakultät für Medizin der Technischen Universität München zur Erlangung des akademischen Grades eines

Doktors der Medizin (Dr.med.)

genehmigten Dissertation.

Vorsitz: Prof. Dr. Marcus Makowski

Prüfer*innen der Dissertation:

1.   apl. Prof. Dr. Norbert Hans Hüser

2.   Priv.-Doz. Dr. Fabian Geisler

Die Dissertation wurde am   11.07.2022   bei der Technischen Universität München eingereicht und durch die Fakultät für Medizin am   11.10.2022   angenommen.

Table of Contents

1 INTRODUCTION

1.1 The basic structure and physiological functions of the liver

The liver is the largest solid organ and the largest gland in the human body. It has many functions, including the formation and excretion of bile, regulation of carbohydrate homeostasis, lipid synthesis and secretion of plasma lipoproteins, formation of proteins, and metabolism/detoxification of foreign substances (Cullen and Stalker 2016).

Anatomically and physiologically, the liver can be divided into four lobes (as shown in Figure 1): left lobe, right lobe, quadrate lobe, and caudate lobe (Chamberlain 2003). The liver has two vessels entering the liver, the hepatic artery and the portal vein, and one vessel leaving the liver, which is the hepatic vein. After entering the liver through the hepatic portal, the hepatic artery and portal vein repeatedly branch into the liver to become interlobular arteries and interlobular veins, which further branch into the hepatic lobules and join the blood sinusoids. The arterial blood and venous blood are mixed in the blood sinusoid, exchange material with hepatocytes, and flow into the central lobular vein, and finally merge in the hepatic vein, which exits the liver and enters the inferior vena cava (Eipel, Abshagen et al. 2010). Lobules are the functional units of the liver. Each lobule is made up of millions of hepatocytes, which are the basic metabolic cell. The various functions of the liver are mainly carried out by hepatocytes.

In addition, as an important digestive organ of the human body, the liver can produce bile and has a rich bile duct system. Primary canalicular bile is produced by hepatocytes, then modified by cholangiocytes and collected from the bile canaliculus to the common hepatic duct via the left and right hepatic ducts. The cystic duct and the common hepatic duct converge to form the common bile duct. Bile stored in the gallbladder finally enters the duodenum through the common bile duct for lipid metabolism and digestion (Strazzabosco and Fabris 2008).
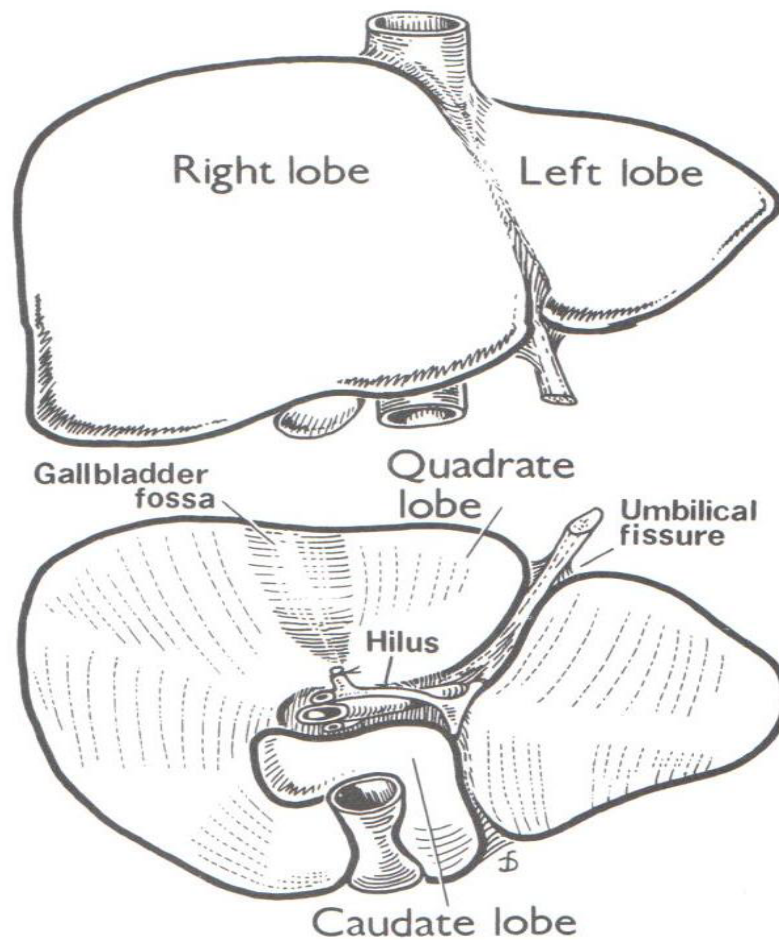
Figure 1. Liver lobe structure (Chamberlain 2003)

1.2 Liver regeneration and its basic processes

The liver can remarkably regenerate itself in response to partial resection or injury (Michalopoulos and DeFrances 1997). After hepatectomy or liver injury, the number of hepatocytes decreases sharply, various feedback signals stimulate the proliferation of hepatocytes in the G0 phase, and the residual liver cells changed from a substantially non-growth state to a rapid growth state through cell proliferation to compensate for lost and damaged liver tissue and restore the physiological functions of the liver. This process is called liver regeneration (LR). At the same time, the body can accurately sense the size of the regenerating liver and stop liver regeneration in time. Liver regeneration is a highly organised tissue regrowth process and is the most important reaction of the liver to injury. The overall process of liver regeneration can be divided

into three phases: priming stage, proliferative phase, and termination phase. Firstly, under stimulation by some cytokines such as TNF-α (tumour necrosis factor alpha) and IL-6 (interleukin-6), quiescent hepatocytes convert from G0 to the G1 phase of the cell cycle. Secondly, with the help of mitogens, hepatocytes go beyond the G1 cell cycle restriction point to the S-phase starting point and then undergo mitosis. Finally, under the influence of some liver regeneration inhibitors, for example, TGF-β (transforming growth factor beta) and activin, hepatocytes terminate the whole proliferation process (Figure 2) (Tao, Wang et al. 2017).
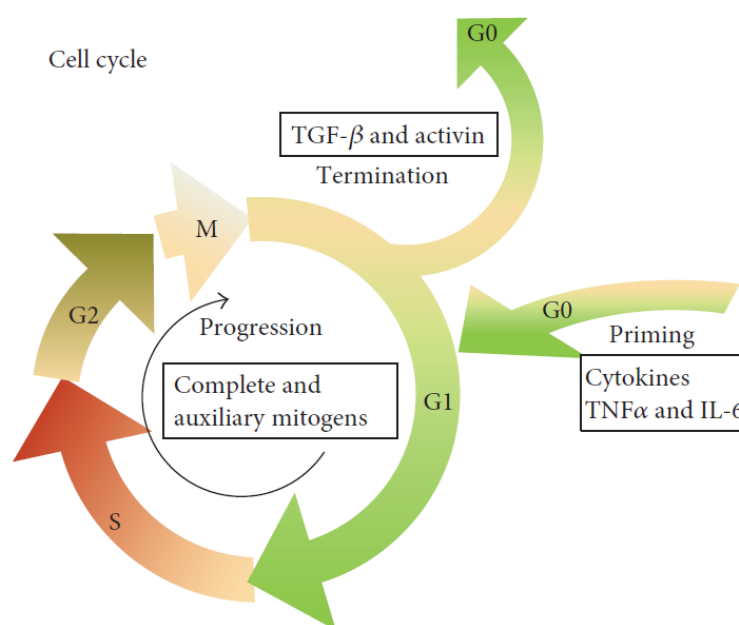
Figure 2. Outline of liver regeneration process (Tao, Wang et al. 2017)

1.3 Gut flora and its physiological functions

The human gut flora, also known as the gastrointestinal microbiota or gut microbiota, is composed of microorganisms normally present in the human intestine. Compared to other areas of the body, the human gut microbiota has the largest number of bacteria and the greatest number of species. There are about 10 trillion bacteria living in the human intestine (Sender, Fuchs et al. 2016). Since we were born, there have been a large number of intestinal flora in the intestine, which play an important role in our

health. The intestinal flora have many crucial physiological functions such as strengthening gut integrity or shaping the intestinal epithelium (Natividad and Verdu 2013), harvesting energy (den Besten, van Eunen et al. 2013), protecting against pathogens (Baumler and Sperandio 2016), and regulating host immunity (Gensollen, Iyer et al. 2016). Moreover, some studies have confirmed a relationship between the intestinal flora and cancer immunotherapy. Routy et al. found that the gut flora played a key role in the effectiveness of immunotherapy. Sampling and analysis of patients with lung and kidney cancer found that patients who did not benefit from immunotherapy lacked a bacterium called *Akkermansia muciniphila* (Routy, Le Chatelier et al. 2018). Matson et al. also found a similar phenomenon that the composition of the commensal microbiota in metastatic melanoma patients is associated with the therapeutic efficacy of immunotherapy (Matson, Fessler et al. 2018).

1.4 Gut microbiota and liver lipid metabolism

The gut microbiota is closely associated with the liver lipid metabolism of the host. Dysbiosis of host gut microbiota affects the body's lipid metabolism in many ways. For instance, the gut microbiota can bio-transform indigestible carbohydrates or dietary fibres in the colon tract into short-chain fatty acids (including acetic acid, propionic acid, iso-butyric acid, butyric acid, isovaleric acid, and valeric acid)(Alexander, Swanson et al. 2019). Among them, acetic acid, propionic acid, and butyric acid are the most important for host lipid metabolism. After being absorbed by the intestine, short-chain fatty acids are converted into acetyl-CoA and propionyl-CoA in the liver and then used as raw materials to participate in glycogen synthesis, gluconeogenesis, and cholesterol synthesis, as well as other metabolic processes, which will eventually affect lipid metabolism in the host (den Besten, Lange et al. 2013).

1.5 The relationship between the gut and the liver

The crosstalk between the gut and liver is increasingly recognised. In fact, there is two-

way communication between the gut and the liver, which is summarised in Figure 3 (Tripathi, Debelius et al. 2018).

1. The liver transports primary bile salts and antimicrobial molecules such as IgA (immunoglobulin A) to the intestinal cavity via the biliary tract, inhibiting microbial overgrowth and maintaining intestinal flora balance.

2. Conversely, very few colonic microbiota-modified secondary bile acids; dietary metabolites such as TMA (trimethylamine), which is converted from choline by intestinal bacteria and can be converted to TMAO (trimethylamine N-oxide), and microbe-associated molecular patterns (MAMPs) are transferred to the liver via the portal vein and influence liver functions.

3. The systemic circulation extends the gut-liver axis. Some inflammatory mediators, liver metabolites from the diet, endogenous or xenobiotic substances such as VLDL (very low-density lipoprotein, a type of lipoprotein cholesterol made by the liver), acetaldehyde, and TMAO are transported to the intestine via the capillary system and have positive (butyrate) or negative (acetaldehyde) effects on the intestinal barrier.
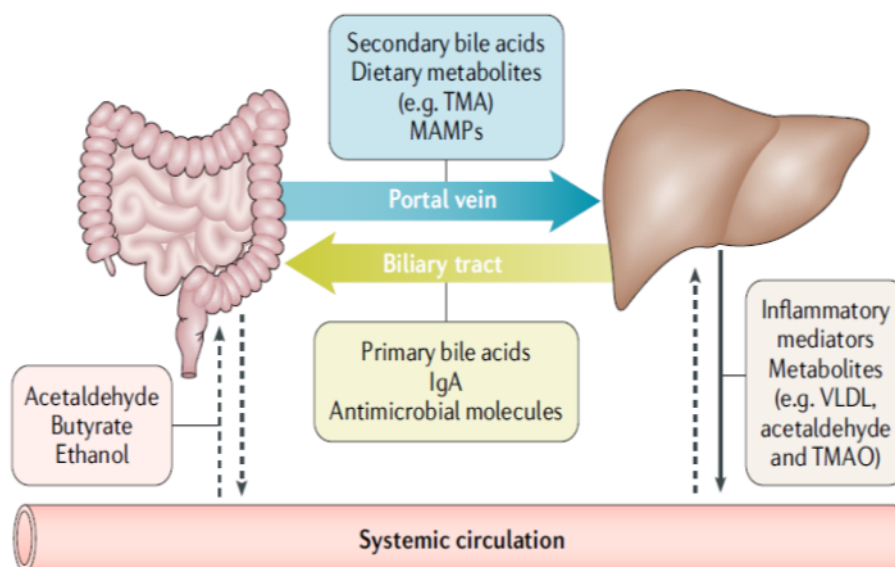

Figure 3. Crosstalk between the gut and the liver (Tripathi, Debelius et al. 2018)

1.6 Liver regeneration mouse models

The animal model of partial hepatectomy was based on a rat hepatectomy experiment performed by Higgins and Anderson in 1931(Higgins 1931). In this experiment, rats were anesthetised, and by making an incision 1-2 cm in length under the xiphoid process, the left and right lobe of the liver were revealed, then the liver pedicle was ligated and the liver lobe was removed along the edge of the ligature. In this way, a 70% partial liver resection model was completed in rats.

A significant difference in liver composition between mice and rats is that mice have a gallbladder, while rats do not. In addition, they also differ in terms of liver volume and the respective lobes. However, mice and rats are similar in the basic liver leaflet structure, branches of the hepatic vein and portal vein, and the biliary system. The earliest and more mature mouse liver resection model was performed by Yokoyama and Wilson in 1952 (Yokoyama, Wilson et al. 1953). This experiment basically used the technique of the classic rat model to ligate and excise the left and middle lobes of the mouse liver. About 65% of the liver lobes were removed. This experiment measured the changes in mouse body weight and liver weight after surgery and monitored liver regeneration after surgery from the perspective of morphology, histology, and biochemistry. It was found that the liver weight of the mice recovered to the preoperative level on the day 8 after the operation. On the day 21, the body weight of the mice returned to the preoperative level.

In recent decades, genetic recombination technology has made a large variety of transgenic mice, and has also been applied to the study of liver regeneration. At the same time, researchers have been working to improve mouse liver resection models. In 2008, Mitchell and Willenbring established a reproducible and easy-to-use 70% excision model in mice with zero intraoperative and postoperative mortality (Mitchell and Willenbring 2008). Thus, the mouse liver regeneration model has basically been standardised and unified.

1.7 Antibiotic treatment mouse models

In order to explore the effects of the microbiota on physiology and disease in humans, two mouse experiment models have been established by researches: germ-free mouse model and antibiotic treatment regimen.

Unlike germ-free conditions, in which mice remain sterile throughout their whole lives, antibiotic treatment can deplete bacteria that have colonised in the mouse intestine since birth. Germ-free mice lack early immune system establishment and development, whereas antibiotic treatment in adult mice specifically allows for the study of the role of bacteria in maintaining cell function and signalling pathways after development. There have also been some studies adding antibiotics to the drinking water of pregnant dams to limit the maternal transfer of microbes and then maintain the cage under antibiotic treatment to study the effects of bacterial depletion early in development (Lamouse-Smith, Tzeng et al. 2011, Deshmukh, Liu et al. 2014, Gonzalez-Perez, Hicks et al. 2016, Li, Hao et al. 2017).

Due to the difference in mechanism of action, different antibiotics can selectively deplete different types of intestinal microbiota. For example, metronidazole and clindamycin both target anaerobes, vancomycin is only effective against Gram-positive bacteria, and polymyxin B specifically targets Gram-negative bacteria (Atarashi, Tanoue et al. 2011, Schubert, Sinani et al. 2015).

Based on this, researchers have used different combinations of antibiotics. Furthermore, the treatment also can differ in term of antibiotic dose and duration of treatment. Normally, antibiotics are diluted in drinking water and some studies also add some sweeteners such as glucose or Splenda to mask any bitterness and ensure that mice drink the antibiotic-containing water (Abt, Osborne et al. 2012, Emal, Rampanelli et al. 2017). Although mice treated with antibiotics are not completely sterile, the reduction in the intestinal flora load has important links with organ function, which can be used for

further research.

1.8 The relationship between gut microbiota, lipid metabolism, and liver regeneration

It is well-known that the gut microbiota plays an important role in regulating host cell proliferation and tissue repair (Tsuei, Chau et al. 2014, Liu, Keane et al. 2015). For example, lipopolysaccharides (LPS) produced by Gram-negative bacteria can stimulate liver regeneration and tissue repair through TLR4 (toll-like receptors 4) (Rakoff-Nahoum, Paglino et al. 2004).

The gut microbiota also affects the metabolic phenotype of mammalian hosts and participates in microbial-host co-metabolism (Martin, Dumas et al. 2007). Changes in the gut microbiota are associated with metabolic disorders (Larsen, Vogensen et al. 2010), metabolic syndrome, obesity (Bäckhed, Ding et al. 2004, Ley, Bäckhed et al. 2005, Ley, Turnbaugh et al. 2006), and non-alcoholic steatohepatitis (Moschen, Kaser et al. 2013).

Cell proliferation increases the energy required for biosynthesising macromolecules and the metabolic needs of precursors, while metabolic disorders inhibit cell proliferation. Therefore, gut microbiota, which is involved in both cell proliferation and lipid metabolism, may have a significant regulatory effect on liver regeneration through lipid metabolism.

There are many extrahepatic molecular signalling networks involved in lipid metabolism that affect liver regeneration, for example, PPARs (peroxisome proliferator-activated receptors) and BAs (bile acids). PPARs are a group of nuclear receptor proteins that act as transcription factors to regulate gene expression (Michalik, Auwerx et al. 2006). This group of nuclear receptor proteins play important roles in cell differentiation, development, metabolism (carbohydrates, lipids, proteins), and carcinogenesis in higher organisms (Berger and Moller 2002, Feige, Gelman et al. 2006,

Belfiore, Genua et al. 2009, Dunning, Anastasi et al. 2014). There are currently three known subtypes of PPARs, namely PPAR-α, PPAR-β, and PPAR-γ (Berger and Moller 2002). Although they share similar sequences, their physiological functions involved in controlling metabolism vary. For instance, PPAR-α mainly regulates fatty acid metabolism, while PPAR-γ participates in adipocyte differentiation. PPAR-β is mostly involved in regulating fatty acid oxidation in muscle fibres (Wang 2010, Grygiel-Górniak 2014).

Moreover, some studies have revealed that PPARs also play important roles in liver regeneration. In particular, Liu et al. found that the lack of activation of PDK1 (phosphoinositide-dependent kinase-1) and E2f (E2 factor) mediated pathways due to PPAR-β deficiency resulted in delayed liver regeneration, which suggests that PPAR-β could regulate liver regeneration by modulating PDK1 and E2f signalling (Liu, Fang et al. 2013). However, Gazit et al. showed that liver regeneration was not suppressed, but rather modestly augmented in liver-specific PPAR-γ null mice maintained on a normal diet. Conversely, disruption of hepatic PPAR-γ expression in mice with diet-induced hepatic steatosis resulted in significant suppression of liver regeneration (Gazit, Huang et al. 2012).

BAs have also been identified as key metabolic signals during liver regeneration, and BAs levels are tightly regulated by the host and gut microbiota (Huang, Ma et al. 2006). There is bidirectional gut-liver axis communication between intestinal microorganisms and BAs (Liu, Keane et al. 2015). On the one hand, the intestinal flora plays a key role in regulating the homeostasis of BAs. On the other hand, BAs can affect the distribution of the intestinal flora.

2 AIMS OF THE STUDY

Liver-extrinsic factors, particularly the gut microbiota and its derived metabolites, have increasingly been recognised as causal contributors to liver regeneration. However, the underlying metabolism mechanisms remain unclear. Accordingly, we studied the importance of the gut-liver axis, and especially the gut microbiota, in a preclinical mouse model.

The aims of this study can be summarised as follows:

(1) To simulate and establish a clinical patient liver surgery model by feeding mice antibiotic-containing drinking water before and after partial hepatectomy.

(2) To explore the relationship between gut microbiota imbalance, liver lipid metabolism, and liver regeneration in mice using this liver resection model.

(3) To look for a new prognostic marker of liver regeneration that can be applied to liver surgery patients.

3 MATERIALS AND METHODS

3.1 Materials

3.1.1 Mouse line

Female C67BL/6 mice aged 10-12 weeks were obtained from Charles River (Sulzfeld, Germany) and housed in specific pathogen-free facilities (ZPF, Klinikum rechts der Isar, Munich, Germany). Mice were used according to the guidelines and regulations. All animal experiments were institutionally approved by the government of Upper Bavaria.

3.1.2 Chemicals and reagents

Chemicals and reagents	Supplier
2-Mercaptoethanol	Sigma-Aldrich, USA
Acrylamide Solution	Carl ROTH, Germany
Ammonium Persulfate (APS)	Sigma-Aldrich, USA
Bovine Serum Albumin (BSA)	Carl ROTH, Germany
Bromophenol Blue	Sigma-Aldrich, USA
Citric Acid	Carl ROTH, Germany
Cell lysis buffer (10×)	Cell Signaling Technology, Germany
DAB + substrate System	Dako, Agilent Technologies, USA
Dulbecco's Phosphate Buffered Saline	Gibco, UK
Dulbecco's Modified Eagle's Medium (DMEM)	Gibco, UK
FBS Superior	Biochrom, Germany
Dimethylsulfoxid (DMSO)	Sigma-Aldrich, USA
Pierce ECL Western Blotting Substrate	Thermo Fisher Scientific, USA
Ethanol	Carl ROTH, Germany
EDTA-free acid	Carl ROTH, Germany

Glycin	Carl ROTH, Germany
Goat Serum	Abcam, UK
Hematoxylin	Merck, Germany
Hydrochloric Acid (HCL)	Carl ROTH, Germany
Hydrogen Peroxide (H_2O_2) (30%)	Carl ROTH, Germany
Histowax	Leica, Germany
Isoflurane CP	CP-Pharma, Germany
L-Glutamine solution	Sigma-Aldrich, USA
Methanol	Carl ROTH, Germany
Milk Powder Blotting Grade	Carl ROTH, Germany
MOPS	Carl ROTH, Germany
Mounting Medium	Vector, USA
Cell Proliferation Kit I (MTT)	Roche, Germany
Opti-MED medium	Gibco, USA
PageRuler Prestained Protein Ladder	Thermo Fisher Scientific, USA
Penicillin-Streptomycin	Gibco, UK
PBS Dulbecco	Biochrom, Germany
RNAse DNAse-free Water	Ambion, USA
Roticlear	Carl ROTH, Germany
Sodium Chloride (NaCl)	Carl ROTH, Germany
SDS Ultra-Pure	Carl ROTH, Germany
SCD1 inhibitor (ab142089)	Abcam, UK
SCD-siRNA (sc36464)	Santa Cruz, USA
Sodium Hydroxide (NaOH)	Carl ROTH, Germany
TEMED	Carl ROTH, Germany
Tris HCl	Sigma-Aldrich, Germany
Tris Base	Sigma-Aldrich, Germany

Tween 20	Sigma-Aldrich, Germany
Trypsin-EDTA solution	Sigma-Aldrich, Germany

3.1.3 Antibiotics and sweetener for mouse treatment

Ampicillin	Sigma-Aldrich, USA
Vancomycin	Sigma-Aldrich, USA
Metronidazole	Sigma-Aldrich, USA
Fluconazole	Sigma-Aldrich, USA
Splenda	TC Heartland, LLC, USA

3.1.4 Kits

NucleoSpin RNA Kit	MACHEREY-NAGEL, Germany
QuantiTect Reverse Transcription Kit	QIAGEN, Germany
KAPA SYBR FAST Kit	Sigma-Aldrich, USA
Lipofectamine RNAiMAX Reagent (2096425)	Thermo Fisher Scientific, USA

3.1.5 Buffers and solutions

Immunohistochemistry buffers

4% Tissue Fix Solution

8% paraformaldehyde	250 mL
Phosphate Buffered Saline	250 mL

20 × Citrate buffer

Citric acid (Monohydrate)	21.0 g

Distilled water	300 mL
Adjust to pH 6.0 with	5M NaOH
Constant volume with distilled water to	500 mL

10x Tris Buffered Saline (10 × TBS)

Tris Base	12.1 g
NaCl	85 g
Distilled Water	800 mL
Adjust pH to 7.4 with	5M HCL
Constant volume with distilled water to	1000 mL

Washing Buffer (1× TBSA)

10×TBS	100 mL
BSA	1 g
Constant volume with distilled water to	1000 mL

Western blotting buffer

1 × SDS lysis Buffer

Glycerol	7.5 mL
10% SDS	15 mL
0.5 M Tris-HCL pH 6.8	6.25 mL
0.5% Bromophenol Blue	1 mL
14.3 M β-mercaptoethanol	2.5 mL
Constant volume with distilled water to	50 mL

Electrophoresis buffer (20 × MOPS)

MOPS	209.2 g
Tris Base	121.2 g
SDS	20 g
EDTA-free acid	6 g
Constant volume with distilled water to	1000 mL

Running buffer (1 ×)

Electrophoresis buffer (20×MOPS)	35 mL
Constant volume with distilled water to	700 mL

Transfer Buffer (10 ×)

Tris Base	30 g
Glycin	144 g
Adjust pH to 8.3 with	5M HCL
Constant volume with distilled water to	1000 mL

Transfer buffer (1 ×)

Transfer Buffer (10×)	100 mL
Methanol	200 mL
Constant volume with distilled water to	1000 mL

Washing Buffer (1 × TBST)

10×TBS	100 mL
Tween 20	1 mL

Distilled Water	800 mL
Constant volume with distilled water to	1000 mL

Blocking buffer

Skimmed milk powder	5 g
Washing buffer	100 mL

3.1.6 List of antibodies

Primary antibodies

Name	Catalog number	Application	Supplier
Cyclin A2	ab181591	WB	Abcam, UK
Cyclin B1	4138S	WB	Cell Signaling Technology,USA
Phospho-RB(Ser807/811)	8516S	WB	Cell Signaling Technology,USA
CDK1	ab131450	WB	Abcam, UK
SCD1(CD.E10)	ab19862	WB	Abcam, UK
SCD1 (C12H5)	2794S	WB	Cell Signaling Technology,USA
Ki67	550609	IHC	BD Biosciences,USA
β-Tubulin	2146S	WB	Cell Signaling Technology,USA
GAPDH	sc32233	WB	Santa Cruz,USA

Secondary antibodies

Name	Catalog number	Application	Supplier
Anti-Mouse IgG HRP Conjugate	W402B	WB	Promega, USA
Anti-Rabbit IgG HRP Conjugate	W401B	WB	Promega, USA
Simple Stain immuno-peroxidase Anti-Mouse	H2011	IHC	N-Histofine, Japan

3.1.7 Laboratory consumables

Name	Supplier
Cotton bud	Lohmann Rauscher, Austria
Cover slips	MENZEL, Germany
Cell culture 10 cm Dish	Corning, USA
Cell culture 75 mL Flasks	Greiner Bio-One, Germany
Cell culture 96-well plates	Corning, USA
96-well PCR microplate, Lightcycler-type	Starlab, Germany
Conical Centrifuge tubes (15mL, 50mL)	Greiner Bio-one, Germany
Microscope Slide	Thermo Scientific, USA
Nitrocellulose Blotting Membranes	Amersham, UK
Single use Syringes(1mL)	Braun, Germany
Sterile needles	BD, USA
Tissue Cassette	Medite, Germany

3.1.8 Laboratory equipment

Name	Supplier
Analytic balance	Sartorius, Germany
Balance	Sartorius, Germany
Centrifuge	Eppendorf, Germany
Cell culture CO_2 incubator	Heraeus, Germany
Electrophoresis / Electroblotting equipment / power supply	Bio-rad, USA
Electrophoresis equipment (large)	Cleaver Scientific Ltd, UK
Freezer -20°C	SIEMENS, Germany
Freezer -80°C	Thermo Scientific, USA
Multiskan FC Microplate Photometer	Thermo Scientific, USA
Incubator 37°C	Thermo Scientific, Germany
Low Voltage Power Supplies	Analytik Jena, Germany
Microscope (Axio)	Zeiss, Germany
Microwave oven	Caso Ecostyle, Germany
Microtome	Leica, Germany
Nanodrop	Thermo Scientific, Germany
PH-meter	Thermo Fisher Scientific, USA
Refrigerator 4°C	LIEBHERR, Switzerland
Real-time PCR amplification and detection instrument (Lightcycler 480)	Roche, Switzerland
Vortex Mixer	NEOLAB, Heidelberg, Germany
UVP ChemStudio	Analytik Jena, Germany
Ultrasound processor	Diagenode bioruptor, Germany
Vacuum tissue processor ASP200s	Leica, Germany
Clean Benches	Heraeus, Germany

Shakers & Mixers	Heidolph, Germany
Tissue embedding machine	Leica, Germany
Tissuelyser II	Qiagen, Germany

3.2 Methods

3.2.1 Antibiotic and Splenda treatment mouse model

For antibiotic treatment, mice received 1 g/L ampicillin, 0.5 g/L vancomycin, 1 g/L metronidazole, 20 mg/L fluconazole, and 1.2% Splenda to block the bitterness of antibiotics in their drinking water for 3 days (72 h) before PHx (partial hepatectomy) and after PHx until sacrifice. Control mice went through the same treatment, but only 1.2% Splenda was added to the drinking water. Drinking water for both groups was changed every three days. All mice were intraperitoneally injected with 100 μL D9-choline 2 h before sacrifice for further analysis.

3.2.2 Partial hepatectomy

Partial hepatectomy (PHx) was performed in 10-12 weeks old female C67BL/6 mice between 10 and 12 AM as previously described (Mitchell and Willenbring 2008). Mice were anesthetised with isoflurane. According to this standard protocol, ligation and resection of the median lobe and the left lateral lobe were performed separately. After different treatment periods, mice were sacrificed. Then, the remnant liver lobes were immediately weighed, fixed in 4% paraformaldehyde or flash-frozen in liquid nitrogen, and stored at -80°C for further genomic and proteomic analysis. The remnant livers, colon content, caecal content, and faeces of mice were collected for further analysis.

3.2.3 Generation of formalin-fixed paraffin-embedded sections

Mouse or human liver tissue samples were fixed in 4% paraformaldehyde at room temperature for 48 to 72 h, then transferred into PBS. The samples were dehydrated in

a graded alcohol series using an automated vacuum tissue processor. Afterwards, the tissue samples were embedded in paraffin blocks and cut with a microtome into 3 μm sections. The sections were moved to an incubator for drying at 37°C overnight.

3.2.4 Immunohistochemistry (IHC) analysis and quantification

Immunohistochemistry staining was performed using the Dako Envision System.

- Paraffin-embedded tissue sections were deparaffinised with Roticlear three times for 10 minutes each, rehydrated with a descending ethanol series (100%, 100%, 100%, 96%, 70%, 50%, 3 minutes each), and then put into dH_2O for 2 minutes.

- Antigen retrieval was performed by treating the slides with citrate buffer (pH 6.0) in a 600W microwave oven for 15 minutes. Then, the slides were cooled down for 20-30 minutes at room temperature.

- The slides were washed in TBSA buffer for 5 minutes and blocked with 3% peroxidase, which was diluted with absolute methanol, for 10 minutes in the dark room. The slides were then washed again in TBSA buffer for three times, 5 minutes each.

- The slides were blocked with TBSA/10% goat serum for 1 h at room temperature.

- The primary antibodies were diluted to the recommended concentrations in PBS, pipetted onto the slides and incubated overnight at 4°C in a humidified slide chamber.

- The slides were washed three times with TBSA for 10 minutes each and then incubated with a secondary antibody for 1 h at room temperature.

- The slides were washed with TBSA three times, for 10 minutes each time. Then the DAB + substrate solution (20 μL DAB in 1 mL substrate buffer) was applied to the slides. The enzymatic reaction was terminated by water when it was ready.

- The slides were counterstained with haematoxylin and rinsed under running tap water for at least 15 minutes.

- The slides were dehydrated in an ascending ethanol series (50%, 70%, 96%, 100%,

100%, 100%, 3 minutes each) and cleared in changed Roticlear three times, for 10 minutes each.

● Finally, the slides were mounted with mounting medium and sealed with a coverslip.

● Images were observed and photographed using an Axio microscope. For quantification, positively stained hepatocyte nuclei in five random high-power microscopic fields were counted and the mean was calculated.

3.2.5 RNA isolation from liver tissue

Total RNA was extracted from mouse liver tissue using NucleoSpin RNA Kit according to the manufacturer's instructions.

The steps are as below:

● 20-40 mg liver tissue of each mouse was weighed with analytical balance and then placed in a 2 mL plastic tube containing 350 μL Buffer RA1 and 3.5 μL β-mercaptoethanol. The liver tissue was homogenised through high-speed shaking using a Tissuelyser II machine. The supernatant was carefully collected, and the rest was discarded.

● The supernatant of homogenised lysate was applied to a NucleoSpin filter with a collection tube (2 mL) and centrifuged for 1 minute at 11,000 × g.

● The filtrate was transferred into a new 1.5 mL microcentrifuge tube. 350 μL ethanol (70%) was added and mixed by vortexing (2 × 5 s).

● Binding RNA. For each preparation, one NucleoSpin RNA column was prepared and placed in a collection tube. The lysate was pipetted up and down 2-3 times and loaded to the column. The columns were centrifuged for 30 s at 11,000 × g and then placed in a new collection tube (2 mL).

● Desalting silica membrane. 350 μL MDB (membrane desalting buffer) was added to the columns and the columns were centrifuged at 11,000 × g for 1 minute to dry the membrane.

- Digesting DNA. The DNase reaction mixture was prepared in a sterile 1.5 mL microcentrifuge tube: for each isolation, 10 μL reconstituted rDNase was added to 90 μL reaction buffer for rDNase. The mixture was mixed by flicking the tube. 95 μL DNase reaction mixture was applied directly onto the centre of the silica membrane of the column and incubated at room temperature for 15 minutes.

- Washing and drying silica membrane.

  First wash:

  200 μL Buffer RAW2 was added to the NucleoSpin RNA column and centrifuged for 30 s at 11,000 × g. Then the column was placed into a new collection tube (2 mL).

  Second wash:

  600 μL Buffer RA3 was added to the NucleoSpin RNA column and centrifuged for 30 s at 11,000 × g. The filtrate was discarded and the column was placed back into the collection tube.

  Third wash:

  250 μL Buffer RA3 was added to the NucleoSpin RNA column and centrifuged for 2 minutes at 11,000 × g to dry the membrane completely. Then, the column was placed into a nuclease-free collection tube (1.5 mL).

- Eluting RNA. The RNA was eluted in 60 μL RNase-free H_2O and centrifuged at 11,000 × g for 1 minute.

  The RNA concentrations were determined using a NanoDrop machine and the RNA samples were stored at -80°C for further analysis.

3.2.6 Complementary DNA reverse transcription

The RNA was reverse-transcribed using the QuantiTect Reverse Transcription Kit according to the instructions.

The steps are described as below:

- The RNA template was thawed on ice and the genomic DNA elimination reaction

was prepared as follow system:

Component	Volume
Template RNA, up to 1 μg	variable
RNase-free water	variable
gDNA wipeout buffer (7×)	2 μL
Total volume	14 μL

The reaction mix was incubated for 2 minutes at 42°C afterwards put on ice immediately.

● The reverse-transcription master mix was prepared on ice as follow system:

Component	Volume
Genomic DNA elimination reaction mix	14 μL
Quantiscript reverse transcriptase	1 μL
Quantiscript RT buffer (5×)	4 μL
RT primer mix	1 μL
Total volume	20 μL

● The reaction mix was incubated at 42°C for 15 minutes and then incubated at 95°C for 3 minutes to inactive Quantiscript reverse transcriptase. The final cDNA was stored at -20°C.

3.2.7 Quantitative real-time PCR (qPCR)

Quantitative real-time PCR (qPCR) was performed in LightCycler 480 real-time PCR machine using KAPA SYBR FAST Kit. The cDNA was diluted 1:5 with the RNase-free water prior to use. The relative mRNA expression levels were quantified against GAPDH or β-actin.

The qPCR reaction component was performed as follows in a 96-well PCR microplate:

Component	Volume
SYBR Green SuperMix	10 μL
Primers	2 μL
cDNA template	5 uL
RNase-free water	3 μL
Total volume	20 μL

List of primers used for qPCR:

Primer name	Forward sense (5' ->3')	Reverse sense (5' -> 3')
Cyclin A2 (Mouse)	CTTGGCTGCACCAACAGT AA	CAAACTCAGTTCTCCCAAA AACA
Cyclin B1 (Mouse)	GCT TAGCGC TGA AAA TTC TTG	TCT TAG CCA GGT GCT GCA TA
Cyclin D1 (Mouse)	TTT CTT TCC AGA GTC ATC AAG TGT	TGA CTC CAG AAG GGCTTC AA
Cyclin E1 (Mouse)	TTT CTG CAG CGT CAT CCT C	TGG AGC TTA TAG ACT TCG CAC A
β-actin (Mouse)	AAG GCC AAC CGT GAA AAG AT	GTG GTA CGA CCA GAG GCA TA
GAPDH (Mouse)	AGG TGG GTG TGA ACG GAT TTG	TGT AGA CCA TGT AGT TGA GGT CA

The qPCR program 'SYBR Green I 96-II' was selected according to the manufacturer's protocol. The data were analysed using LightCycler 480 v1.5 software.

3.2.8 Cell culture

The human HCC (hepatocellular carcinoma) cell line HepG2 was purchased from American Tissue Culture Collection (ATCC, Manassas, VA). HepG2 cells were cultured in Dulbecco's Modified Eagle Medium, 1% L-glutamine with 10% foetal bovine serum, and 1% penicillin/streptomycin at 37°C in a 5% CO_2 cell culture incubator.

3.2.9 Cell transfection assay

The 4×10^5 HepG2 cells were seeded in 6-well plates one day before transfection. Lipofectamine RNAiMAX transfection reagent was used to transfect according to the manufacturer's instructions as follows:

- 9 µL lipofectamine RNAiMAX reagent was diluted in 150 µL Opti-MEM medium.

- 5 µL SCD-siRNA or 5µl control siRNA was diluted in 150 µL Opti-MED medium.

- Diluted SCD-siRNA or control siRNA was added to diluted lipofectamine RNAiMAX Reagent (1:1 ratio) and the complex was incubated for 5 minutes at room temperature.

- SCD-siRNA or control siRNA complex was added to the cells. The cells were incubated for 48 h at 37°C.

After 48 h, cells were harvested for further analysis.

3.2.10 Immunoblot analysis

Protein extraction from liver tissue

- A piece of frozen liver tissue weighing 20-40 mg was lysed in 400-800 µL 1×SDS lysis buffer in a 2 mL tube on ice.

- The liver samples were disrupted using Tissuelyser II with metal beats for 3 minutes.

- The liver samples were transferred to an ultrasound processor (Diagenode

bioruptor) for sonification for 5 minutes.

- The liver samples were put on ice and centrifuged at high speed briefly.

- The supernatant of liver samples was transferred to a new 1.5 mL tube.

- The liver samples were heated for 5 minutes at 95°C and stored at 20°C.

Protein extraction from cultured cells:

- The medium of HepG2 cells was aspirated off and the cells were washed with 10 mL DPBS.

- 2.5 mL Trypsin-EDTA solution was added to the HepG2 cells. The cells were put in a 37°C incubator for about 10 minutes until the cells were loose. The plate was tapped to help cells come off of the plate.

- Then, 8 mL DMEM was added to the plate and the cells were resuspended.

- The HepG2 cells were transferred to a 15 mL tube and centrifuged at 1500 rpm for 4 minutes at room temperature.

- Then, HepG2 cells were washed with 5 mL DPBS and resuspended well in 150 μL lysis buffer.

- Then, HepG2 cells were transferred to an ultrasound processor (Diagenode bioruptor) for sonification for 5 minutes.

- 150 μL 1×SDS lysis buffer was added to the cell samples and then the samples were boiled at 95°C for 5 minutes and stored at -20°C.

SDS-polyacrylamide gel electrophoresis (SDS-PAGE):

- The protein samples were heated at 60°C for 5 minutes. The separating and stacking gels were made as follows:

Lower separating gel (10% for two gels)

| H_2O | 4.1 mL |
| Acrylamide 30% | 3.3 mL |

Tris-HCl 1.5M pH8.8	2.6 mL
SDS 10%	100 μL
APS 10%	50 μL
TEMED	15 μL
Total volume	10 mL

Upper stacking gel (10% for two gels)

H_2O	3 mL
Acrylamide 30%	750 μL
Tris-HCl 1.5M pH8.8	1.3 mL
SDS 10%	50 μL
APS 10%	25 μL
TEMED	10 μL
Total volume	5 mL

- Two SDS-PAGE gels were put in electrophoresis equipment and filled with 750 mL 1× running buffer.

- 15 μL of each sample and 3 μL of protein molecular weight markers were loaded into each well of the SDS-PAGE gels. The proteins were separated by gel electrophoresis in running buffer at 80 V for around 30 minutes, and then the voltage was increased to 110 V until finish.

- The protein from the gel to the membrane: the proteins were transferred from the gel onto a nitrocellulose membrane using an electroblotting equipment (Trans-Blot SD Wet Transfer Cell) on ice. The protein was transferred over 1.5 h at 300 mA.

- The membrane was blocked with 5% non-fat milk for 1 h at room temperature to avoid the non-specific antibodies binding.

- The membrane was washed with TBST three times for 3 minutes each and then

incubated with the primary antibodies diluted with BSA solution on a shaker overnight at 4°C.

- On the second day, the membrane was washed with TBST three times for 5 minutes each. Then the membrane was incubated with secondary antibody diluted with 5% non-fat milk for 1 h on a shaker at room temperature. Finally, the membrane was washed again with TBST three times for 5 minutes each.

- Detection of protein: the membrane was incubated with the mixture of Pierce ECL Western Blotting Substrate for signal development. The protein signal was detected using the UVP ChemStudio system (Analytik Jena). The relative protein expression levels were analysed using ImageJ image analysis software (https://imagej.nih.gov/ij/).

3.2.11 MTT assay

To evaluate the influence of SCD1 (stearoyl-CoA desaturase1) on cell proliferation, the MTT (3-(4,5-dimethylthiazol-2-yl)-2,5-diphenyltetrazolium bromide) assay was performed in HepG2 cells after SCD1 inhibitor treatment.

The HepG2 cells were seeded at a density of 2×10^3 cells per well in a 96-well plate with a complete medium 24 h before treatment.

- Then HepG2 cells were treated with 10μM SCD1 inhibitor or 1‰ DMSO control medium for 24, 48, 72, and 96 h.

- 20 μL MTT reagent was added to the cells and the 96-well plate was put in a 37°C incubator for 4 h.

- After 4 h, the 96-well plate was taken out and 150 μL DMSO was added. Then, the plate was shaken in a dark room for 10 minutes.

- The absorbance of each well was read at 570 nm using a Multiskan FC Microplate Photometer (Thermo Scientific) system according to the manufacturer's instructions.

3.2.12 Statistical analysis

All statistical analysis was performed using GraphPad Prism 8.0 (GraphPad, San Diego, USA). Variations were indicated by using the standard error presented as mean ± SEM. Statistical differences were analysed using the two-tailed unpaired or paired Student's t-test or the Mann-Whitney U test. The Kaplan-Meier method was used in the survival analysis. Linear regression was used in the correlation analysis. A P-value less than 0.05 was considered to be a significant difference. Statistically significant differences are displayed as *$P < 0.05$, **$P < 0.01$, ***$P < 0.001$, ****$P < 0.0001$.

4 RESULTS

4.1 Oral antibiotic therapy seriously impairs regeneration of the liver and the survival rate after PHx

To evaluate whether liver regeneration is affected by oral antibiotic therapy, the mouse liver weight to body weight (liver/body weight) ratio was determined and Ki67 immunohistochemistry staining was performed using liver tissue after PHx in control or antibiotic-treated mice to assess liver recovery over time. At first, we measured the liver/body weight ratio of mice just after PHx (0 h), and showed that mice in the antibiotic-treated group had a significantly lower value than the control group (Figure 4A). To eliminate the influence of that at the beginning, we calculated a normalised liver/body weight ratio in the following timepoints. Mice treated with antibiotics had a significantly reduced liver/body weight ratio at 24, 48, 72, and 96 h after PHx compared to control mice (Figure 4B). Antibiotic treatment was carried out as described in 3.2.1.
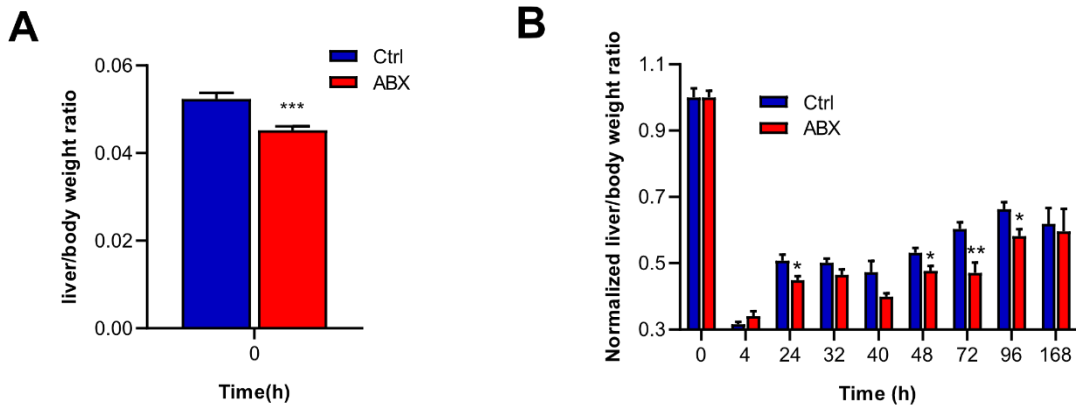
Figure 4. Liver/body weight ratio and normalised liver/body weight ratio

Liver/body weight ratio (A) and normalised liver/body weight ratio (B) were determined and calculated at 0 h and following timepoints after PHx (n=5-10 mice per timepoint in each group). Data were analysed using the two-tailed unpaired Student's t-test or the Mann-Whitney U test. Data are presented as mean ± SEM. *P < 0.05, **P < 0.01, ***P < 0.001. ABX: antibiotic treatment group, Ctrl: control group.

Following partial hepatectomy, some antibiotic-treated mice did not survive to the preset long experimental endpoints (for example 96 h and 168 h). Therefore, we wondered if the antibiotic treatment has an influence on the survival of mice after surgical intervention. We performed a survival analysis showing that, compared to control mice, antibiotic-treated mice did not tolerate the PHx well and showed significantly higher mortality before reaching the experimental endpoint (Figure 5).
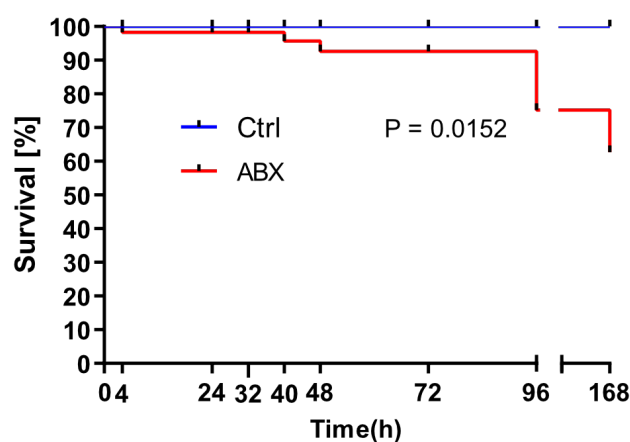

Figure 5. Survival rate in antibiotic-treated and control mice after hepatectomy
Survival was estimated by the Kaplan-Meier method, and the differences in survival rate were evaluated with a log-rank test. Data are presented as mean ± SEM.

The Ki67 protein, as a widely used cellular marker for proliferation, is present during all active phases of the cell cycle (G1, S, G2, and mitosis) (Bruno and Darzynkiewicz 1992). Accordingly, anti-Ki67 immunohistochemistry staining was performed in mouse liver sections. The results show that antibiotic-treated mice displayed a significant decrease in the number of Ki67-positive hepatocytes per field at 32, 40, 48, and 72 h, but had a significantly higher number at 168 h after PHx (Figure 6, 7), which suggests that hepatocytes proliferation was delayed in mice due to the effects of antibiotic treatment. In conclusion, these data suggest that oral antibiotic therapy disrupts the homeostasis of the gut microbiota, and as a consequence, liver regeneration in mice and post-hepatectomy survival are affected.
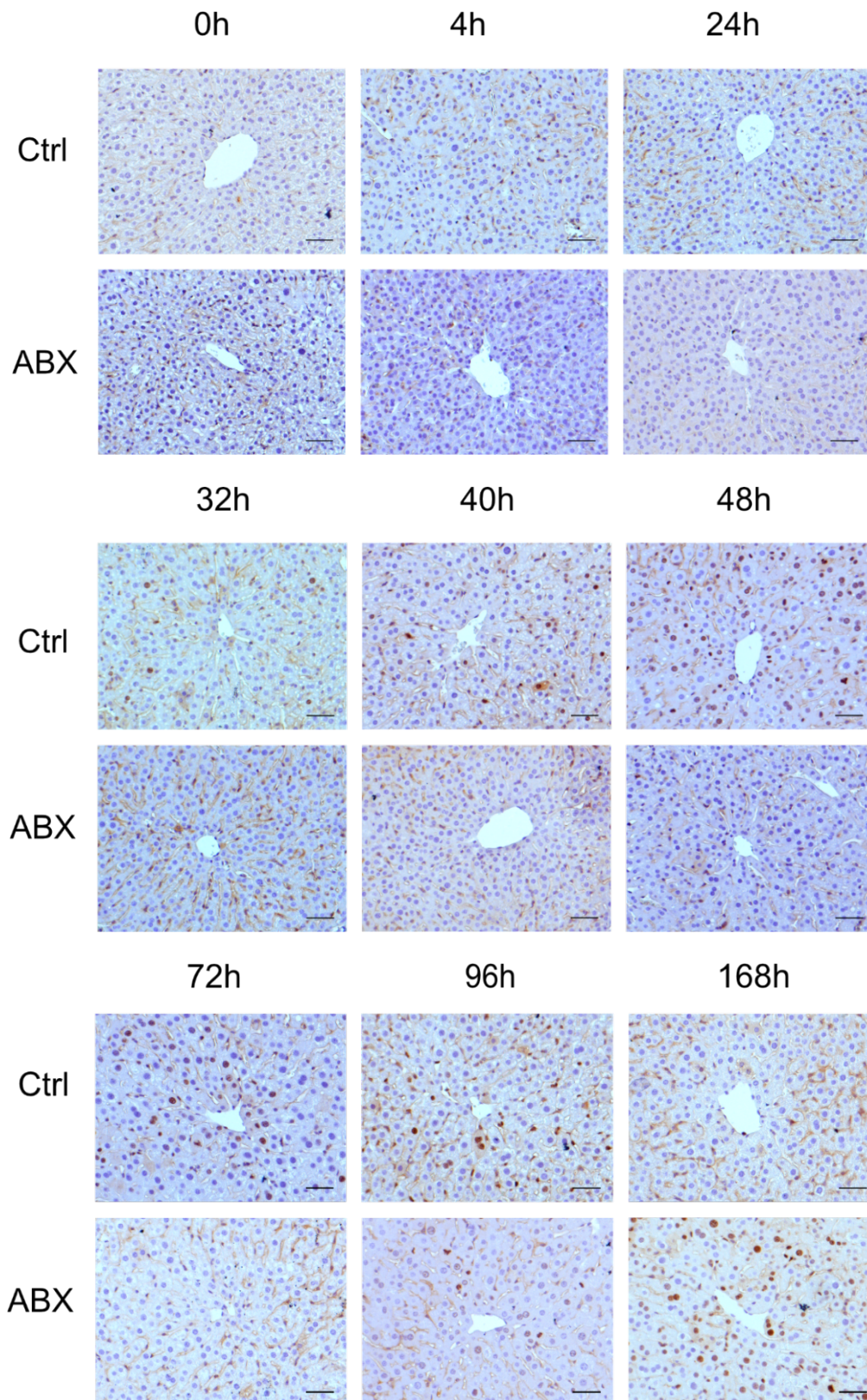
Figure 6. Representative immunohistochemical images for Ki67 in the mouse liver

The expression of Ki67 in the mouse liver in different groups after PHx was detected using IHC staining; representative images are shown above (Scale bars: 50 μm).
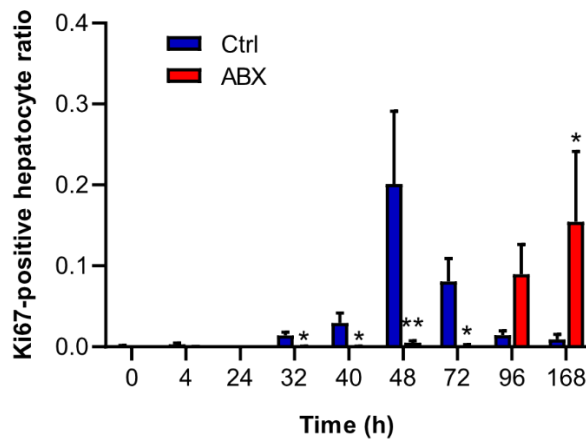
Figure 7. Quantification of Ki67-positive hepatocytes in the mouse liver at different timepoints after PHx

Data were analysed using the two-tailed unpaired Student's t-test or the Mann-Whitney U test. Data are presented as mean ± SEM. *P < 0.05, **P < 0.01.

4.2 Induced dysbiosis of gut microbiota affects liver cell cycle regulators after PHx

To investigate the mechanisms underlying impaired liver regeneration in antibiotic-treated mice after PHx, the mRNA levels and protein expression of various cell cycle regulators were determined. As shown in Figure 8A and 8B, mRNA levels of cyclin D1 and E1, which are responsible for the late G1-phase of the cell cycle, were decreased in antibiotic-treated mice compared to control mice from 0 to 40 h and 32 to 40 h after PHx.

Moreover, the mRNA levels of the regulator cyclin A2 and B1, which are effective in the S and G2 phase of the cell cycle, respectively, were significantly reduced in antibiotic-treated mice compared with control mice from 0 to 72 h except for 40 h and 72 h regarding cyclin B1 after PHx (Figure 8C, D).
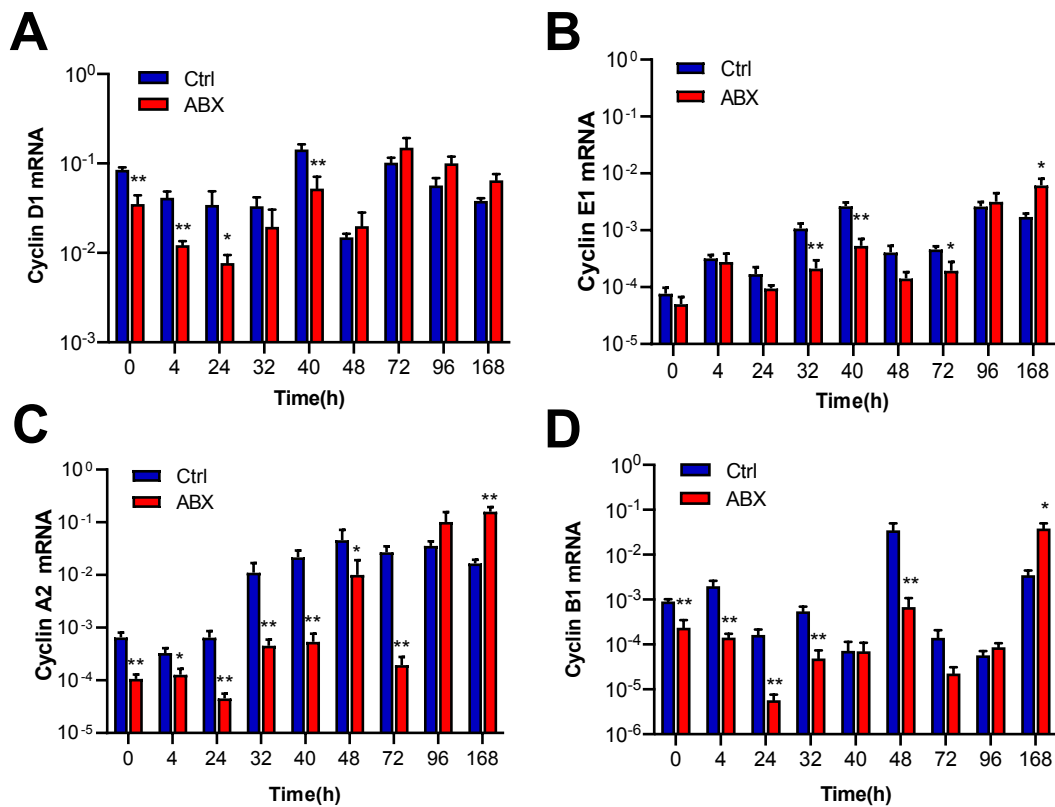
Figure 8. Relative hepatic mRNA levels of cyclin D1, E1, A2, and B1 in two groups of mice after PHx

Hepatic mRNA levels of cyclin D1 (A), E1 (B), A2 (C), and B1 (D) in antibiotic-treated mice were normalised to GAPDH and compared with control mice. Data were analysed using the two-tailed unpaired Student's t-test or the Mann-Whitney U test. Data are presented as mean ± SEM. *P < 0.05, **P < 0.01.

In addition to the detection of cell cycle regulators at the mRNA level, the protein expression of cyclin A2 and B1 was further confirmed by western blot. In agreement with the mRNA results, the expression of cyclin A2 and B1 was markedly diminished in antibiotic-treated mice compared to control mice from 40 to 72 h and at 48 h timepoint after PHx, respectively (Figure 9,10).
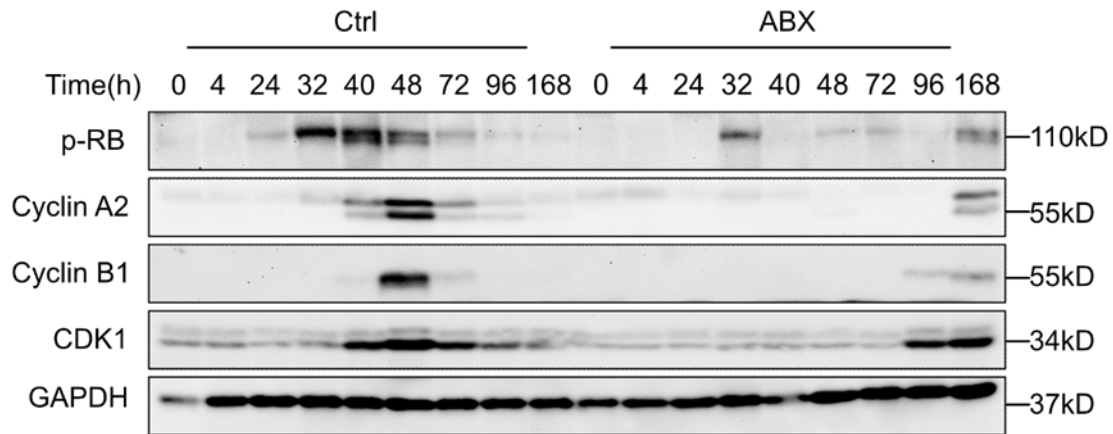
Figure 9. Protein expression of different cell cycle regulators in the mouse liver

The protein levels of phosphorylated-RB, cyclin A2, cyclin B1, and CDK1 at the indicated timepoints after PHx were analysed by Western blot. Representative gels are depicted.
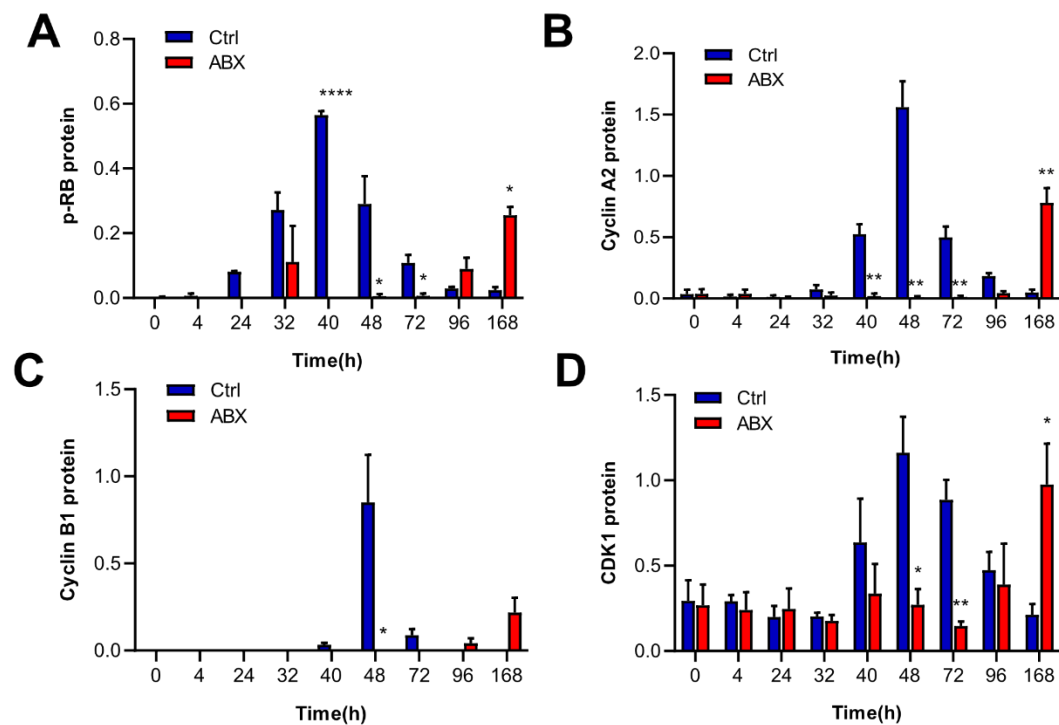

Figure 10. Quantification of mouse hepatic protein expression of p-RB, cyclin A2, cyclin B1, and CDK1

Data were pooled from at least three independent experiments and were analysed using the two-tailed unpaired Student's t-test or the Mann-Whitney U test. Data are presented as mean ± SEM. *P < 0.05, **P < 0.01, ****P < 0.0001.

Furthermore, the protein expression level of p-Rb, which is required in the process beyond the G1/S restriction point in the cell cycle, was also tested. The results show that phosphorylation of Rb protein was strongly diminished in the liver of antibiotic-treated mice from 40 to 72 h after PHx (Figure 9, 10).

Based on the above results, the expression of another relevant cell cycle regulator CDK1 (cyclin dependent kinase1), which is activated by cyclin A2 and B1 and acts as an essential driver of the cell cycle, was also examined using western blot. In accordance with the results on cyclin A2 and B1, the downregulation of CDK1 expression was also found in antibiotic-treated mice from 40 to 72 h after PHx (Figure 9, 10).

Of note, the mRNA levels of cyclin E1, cyclin A2 and cyclin B1, as well as the protein expression of cyclin A2, CDK1, and p-RB, was found to catch up at the late timepoint after PHx in antibiotic-treated mice, and showed a significant increase at the 168 h timepoint (Figure 8B, C, D; Figure 9; Figure 10A, B, D). This is consistent with earlier research showing that liver regeneration is delayed after PHx in antibiotic-treated rats, as well as germ-free and lipopolysaccharide-resistant mice, suggesting that the products of the gut microbiota are responsible for promoting liver regeneration after PHx (Cornell 1985, Cornell, Liljequist et al. 1990).

Taken together, these results indicate that induced dysbiosis of the gut microbiota by oral antibiotics impedes hepatocyte proliferation in mice by affecting liver cell cycle regulators after PHx.

4.3 Lipid metabolising enzyme SCD1 promotes cell proliferation in vitro

Based on our previous results (Anna Sichler, AG Janssen, Department of Surgery, Technische Universität München, personal communication), oral antibiotics in drinking water affects the lipid content and synthesis in mice and results in a down-regulation of the lipid enzyme SCD1 (stearoyl-CoA desaturase1) in the mouse liver.

To further confirm the relationship between the lipid metabolising enzyme SCD1 and hepatocyte proliferation in vitro, an MTT assay and cell transfection were conducted in human hepatoma HepG2 cells.

Firstly, we interfered with SCD1 expression by transferring control SCD-siRNA to HepG2 cells in vitro. Then, western blot was performed on the cells 48 h after transfection. As shown in Figure 11A and B, not only the expression of SCD1 but also the expression of the cell cycle regulator cyclin A2 were significantly decreased compared to the control group.

To verify the effect of SCD1 on cell proliferation, an MTT assay was carried out in HepG2 cells. The principle of MTT (3-(4,5-dimethylthiazol-2-yl)-2,5-diphenyltetrazolium bromide) detection is that the succinate dehydrogenase in the mitochondria of living cells can reduce exogenous MTT to the water-insoluble blue-purple crystal formazan and deposit it in cells, while dead cells have no such function (Mosmann 1983, Vistica, Skehan et al. 1991). Dimethyl sulfoxide (DMSO) can dissolve formazan in cells, and its light absorption value is measured at a wavelength of 500-600 nm with an enzyme-linked immunoassay, which can indirectly reflect the number of living cells. Within a certain range of cell number, the amount of MTT crystal formation is proportional to the number of cells. This method has been widely used to measure cellular metabolic activity as an indicator of cell viability, proliferation, and cytotoxicity.

From the results of the experiment (Figure 11C), the absorbance value at 570 nm of the SCD1 inhibitor treated group was significantly lower than that of the control group at 48, 72, and 96 h after treatment, which indicates that the SCD1 inhibitor could decrease the cell proliferation of HepG2 cells. This part of the results shows that SCD1 is essential to hepatoma cell proliferation in vitro.
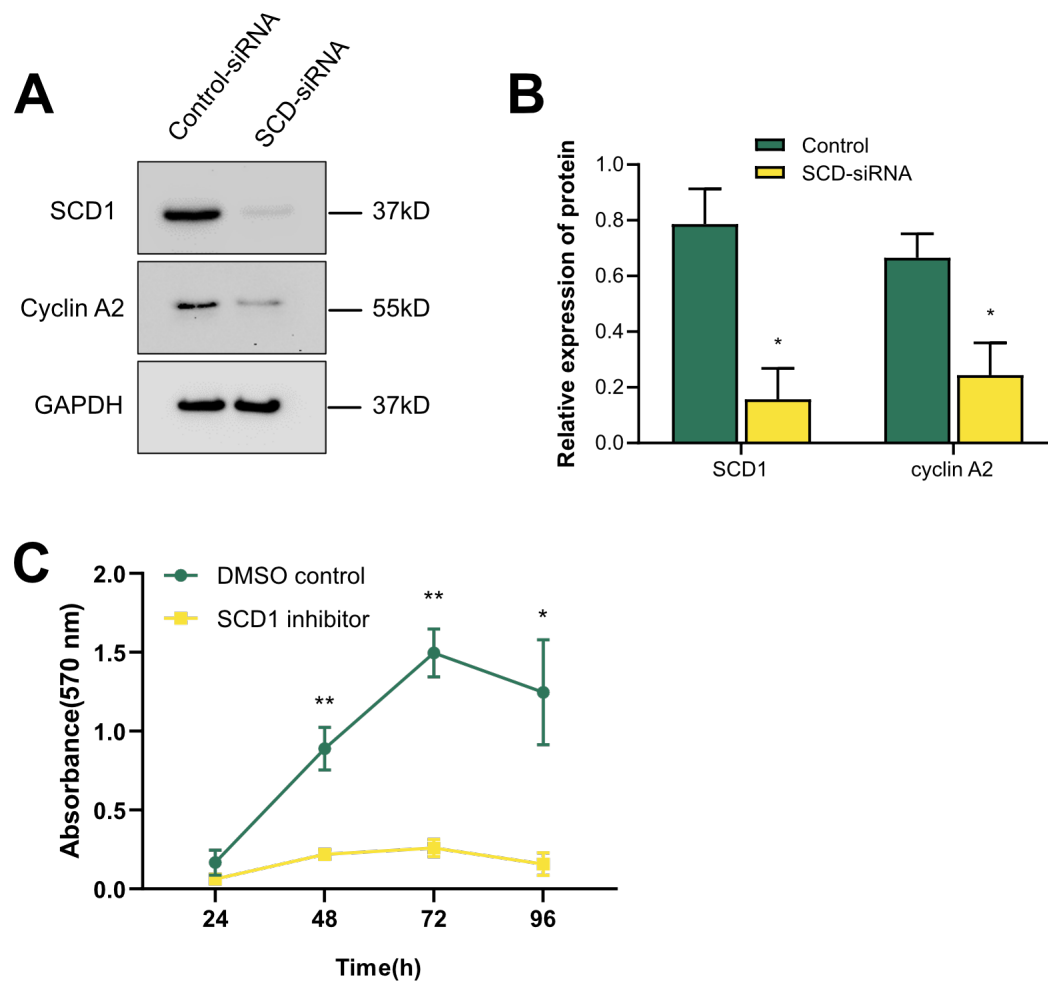
Figure 11. The promoting effect of SCD1 on cell proliferation in vitro
(A) SCD1 and cyclin A2 protein expression in HepG2 cells after transfection with control siRNA or SCD-siRNA determined by western blot using GAPDH as a loading control. (B) Quantification of mouse hepatic protein expression of SCD1 and cyclin A2 using ImageJ. (C) An MTT assay was conducted to assess cell viability at 24, 48, 72 and 96 h in HepG2 cells after being treated with an SCD1 inhibitor (10 µM) or DMSO control. Data are shown as the absorbance of triplicate measurements. Data were analysed using the two-tailed unpaired Student's t-test or the Mann-Whitney U test and presented as mean ± SEM. *$P < 0.05$, **$P < 0.01$.

4.4 The regenerating liver tissue of patients highly expresses SCD1

After completing the mouse partial hepatectomy model and in vitro experiments, we went further to examine the correlation of the key metabolic enzyme SCD1 and liver

regeneration in patients. Therefore, we selected three patients who had undergone preoperative ALPPS (associating liver partition and portal vein ligation for staged hepatectomy) intervention before liver surgery.

First of all, to safely perform liver resection, preoperative ALPPS treatment was applied in patients with insufficient FRL (future remnant liver) as described previously (Popescu, Alexandrescu et al. 2017). After 7 to 14 days, FRL volumetry was measured by CT scan to determine that if the liver had grown enough to safely perform a liver resection, then the part of the liver with the tumour was removed by the surgeon. Meanwhile, one piece of tissue from the embolised part of the liver and new growth part of the liver in the patient was cut off and labelled as hypotrophy or hypertrophy, respectively, for further analysis.

Moreover, the expression of the key fatty acid metabolism enzyme SCD1 was determined in the liver samples and compared by western blot. The results indicate that the expression of SCD1 in the hypertrophy of the liver tended to be higher than that in the hypotrophy of the liver in all three patients (Figure 12A and B). Interestingly, through the evaluation of liver regeneration volumetry by CT scanning and calculation of the liver regeneration index of the three patients (Melanie Laschinger and Fabian Lohöfer, Department of Surgery, Technische Universität München, personal communication), we found that patient 1, who had the highest expression of protein SCD1 in liver of the three patients, also had the highest regeneration index post-ALPPS intervention (Figure 12C).

To further investigate the relationship between the lipid metabolism enzyme SCD1 and liver regeneration in the three patients, we performed a correlation analysis regarding the regeneration index and the expression of protein SCD1 in the hypertrophic liver the three patients. Due the limited number of patients, there is no significant correlation between these parameters (Figure 12D).
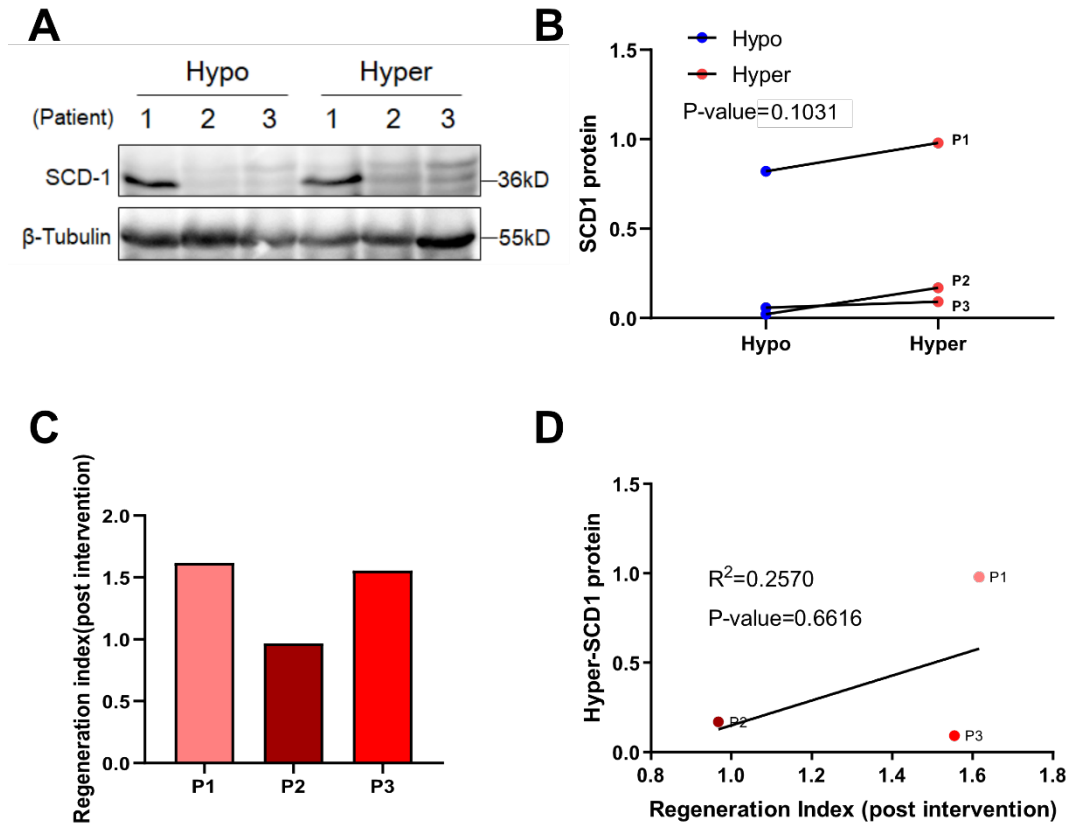
Figure 12. The expression of SCD1 in human liver tissue and its relationship with liver regeneration

(A) The protein expression of SCD1 in the hypotrophy and hypertrophy in three patients' livers was determined by western blot. (B) Quantification of protein expression of SCD1 in the hypotrophy and hypertrophy of three patients' livers. (C) Regeneration index of three patients' livers post-intervention. (D) Correlation analysis of SCD1 expression with the liver regeneration index of hypertrophic part in three patients' liver post-intervention. Correlations were analysed by linear regression. Statistical significance was analysed using a paired two-tailed Student's t-test. Data are presented as mean ± SEM. Hypo: hypotrophy, Hyper: hypertrophy, P1: patient 1, P2: patient 2, P3: patient 3.

5 DISCUSSION

5.1 A mouse model to simulate clinical antibiotic treatment

In the present study, we performed a mouse model that simulated some features of clinical perioperative antibiotic therapy during liver surgery. Under normal circumstances, patients who undergo liver surgery are not recommended to use antibiotics to prevent infection. Some randomised controlled trials also showed that antibiotic prophylaxis after liver resection is unnecessary (Hirokawa, Hayashi et al. 2013). However, we know that the liver is not only a metabolic organ but also an important immune organ of the human body (Parker and Picut 2005, Racanelli and Rehermann 2006, Robinson, Harmon et al. 2016). Liver disease, especially in patients with end-stage cirrhosis, is usually accompanied by liver insufficiency, which further causes the decline of the function of the body's immune system. Consequently, there are situations in which antibiotics are needed to prevent or treat infection in the perioperative treatment of clinical liver surgery patients; this is the purpose of our study. We aim to simulate the situation of these patients through experimental antibiotic-treated mice to further evaluate liver regeneration.

5.2 The effect of antibiotic administration on the mouse gut microbiota

In order to induce the dysbiosis of mice gut microbiota, we treated mice with drinking water with or without antibiotics during the period around partial hepatectomy in our study. Regarding the duration of antibiotic treatment, some studies have found that total microbiota load and diversity in the gut is dramatically reduced, particularly after several days of antibiotic treatment, but recovers after three to four weeks in mice and humans (De La Cochetiere, Durand et al. 2005, Puhl, Uwiera et al. 2012, Panda, El khader et al. 2014). Moreover, it has also been shown that antibiotic treatment causes obvious enlargement of the cecum in mice and an increase in the overall length of the intestine, which is concordant with what we observed in our treated mice. However,

there were no pathologic changes related to increased caecal size or length of the intestine (Puhl, Uwiera et al. 2012). In some similar research models, mice were orally administered antibiotics for four weeks (Wu, Sun et al. 2015). Comparatively, we did not treat the mice with antibiotics for that long, but chose a short-term treatment period of three days before PHx. After that, we determined the diversity and composition of microbial communities in the caecal content of mice on the basis of 16S rRNA sequences, as the cecum plays a vital role in microbial fermentation and the production of volatile fatty acids in mice (Eyssen and Parmentier 1974, Hedrich 2004). More importantly, the mouse cecum is crucial for maintaining a normal microbial equilibrium in the large intestine, which is important for achieving colonisation resistance (Voravuthikunchai and Lee 1987). As expected, antibiotic administration significantly altered the caecal microbiota composition at the phylum level and decreased the diversity of the microbiota in mice compared with the control group, which suggests that our mouse model successfully induced severe dysbiosis of the gut commensal microbiota in mice (Anna Sichler, AG Janssen, Department of Surgery, Technische Universität München, personal communication).

5.3 The effect of antibiotic administration on the SCFAs content in the mouse colon and the synthesis of phosphatidylcholine

In our study, we found that, after three days of antibiotics combination treatment, the major perturbation of the microbial component showed a conspicuous decrease in the composition ratio of Firmicutes and Bacteroidetes, but an increased composition ratio of Cyanobacteria (Anna Sichler, AG Janssen, Department of Surgery, Technische Universität München, personal communication).

Based on a previous study (Blaut and Clavel 2007), we know that short-chain fatty acids (SCFAs), including acetic, propionic, and butyric acid, are the principal end products of fermentative metabolism by human colon bacteria. Furthermore, for example, there are also some studies showing that butyrate-producing bacteria are present in several

different classes within the Firmicutes (Louis and Flint 2009, Louis, Young et al. 2010), whereas acetate and propionate are mainly produced by Bacteroidetes (Levy, Thaiss et al. 2016, Feng, Ao et al. 2018). Remarkably, those two are indeed the kinds of bacteria that were notably decreased in the composition ratio at the phylum level when we checked the relative abundance of colon content bacteria in antibiotic-treated mice compared to the control mice.

Different SCFAs perform various biological functions in the host. For instance, butyric acid is the main energy substance of colonic epithelial cells (Cummings, Pomare et al. 1987, Al-Lahham, Peppelenbosch et al. 2010), and acetic acid often participates in the production of cholesterol and fatty acid precursors, while propionic acid is mainly involved in gluconeogenesis in liver and intestines (Delzenne and Williams 2002, De Vadder, Kovatcheva-Datchary et al. 2014). Although several studies have releveled that SCFAs have a stimulatory effect on epithelial cell proliferation in the large intestine in rats (Sakata and Von Engelhardt 1983, Ichikawa, Shineha et al. 2002), their potential directly contributions to liver regeneration still need to be further investigated.

Accordingly, we queried how the SCFAs content changes in the mouse colon after antibiotic treatment. As determined by GC-MS/MS, we found that nearly the entire SCFAs content in the mouse colon was significantly decreased compared with the control group at early timepoints after PHx (Josef Ecker, ZIEL-Institute for Food and Health, Technische Universität München, personal communication).

Phospholipids are the main fundamental component of the cell membrane, PC (phosphatidylcholine) represents about half of the membrane phospholipid content (Esko and Raetz 1980, Sharma, Ghosh et al. 2017). Cell membrane growth occurs throughout much of the cell cycle and is an indispensable part of cell proliferation (Tzur, Kafri et al. 2009, McCusker and Kellogg 2012). Therefore, we also measured the PC level with labelled D9-choline between the antibiotic-treated and control groups. We found that newly synthesized PC was significantly reduced in antibiotic-treated group

compared to the control group (Josef Ecker, ZIEL-Institute for Food and Health, Technische Universität München, personal communication).

As the most abundant constituent of cell membranes, PC is an important support nutrient for all known cell types, including hepatocytes (Alberts, Johnson et al. 2002). The wide range of liver functions, as well as its capacity for ongoing renewal, depends on its ability to make new cell membranes, which are on average 65% PC (Kidd 1996). Taken together, we drew the conclusion that antibiotic administration impaired liver regeneration indirectly by affecting the content of SCFAs and newly synthesised PC.

5.4 The effect of antibiotic administration on fatty acid metabolism enzymes and the influence of SCD1 on hepatoma cell proliferation in vitro

To our knowledge, the structure of PC (phosphatidylcholine) consists of a choline head group, a glycerophosphoric acid, and two fatty acids which include one saturated fatty acid and one unsaturated fatty acid. As the key enzymes required for fatty acid metabolism, FASN (fatty acid synthase), SCD1, and ELOVL6 (elongation of very long chain fatty acids protein 6) play vital roles in the biosynthesis process of saturated fatty acids and unsaturated fatty acids in mammals (Guillou, Zadravec et al. 2010). Hence, we hypothesised that antibiotic treatment affects the level of these enzymes in the mouse liver.

To test our conjecture, we assessed the mRNA levels of FASN, ELOVL6, and SCD1, as well as the protein expression of SCD1. The results showed that, except for FASN and ELOVl6, the mRNA level and the protein expression of SCD1, were dramatically decreased in antibiotic-treated mice at early timepoints after PHx compared to control group mice. Taken together, these results suggest that antibiotic administration impairs mouse liver regeneration indirectly through an effect on SCD1 level (Anna Sichler, AG Janssen, Department of Surgery, Technische Universität München, personal communication).

As a key enzyme in fatty acid metabolism, SCD1 has been found to play important roles in a variety of digestive system cancers, including liver cancer. For example, some findings show that SCD1 promotes metastasis of colorectal cancer cells through monounsaturated fatty acids production and suppressing PTEN (phosphatase and tensin homolog) in response to glucose (Ran, Zhu et al. 2018) and promotes gastric cancer stem cell stemness through the Hippo/YAP (Yes-associated protein) pathway (Gao, Li et al. 2020). Huang et al. found that inhibition of SCD1 impairs cell proliferation and triggers autophagy-induced apoptosis in human HCC cells via AMPK (AMP-activated protein kinase) activation (Huang, Jiang et al. 2015). Consistently, we also confirmed the essential function of SCD1 for human hepatoma HepG2 cell proliferation in vitro in our study. Although we also performed SCD-siRNA transfection assays in the mouse hepatocyte cell line AML-12, there was no difference between the experimental and control groups regarding the expression of cell proliferation markers (data not shown). Given that little research has been done in this area, more investigations are needed in the future.

5.5 The relationship between SCD1 and liver regeneration in patients

Hepatectomy has developed as an effective oncologic treatment for many primary liver malignancies and metastatic liver tumours. If possible, hepatectomy could provide the best survival outcome in many clinical situations. However, many patients with primary hepatocellular carcinoma require extensive hepatic resection due to the large size of the tumour adjacent to important vascular structures, resulting in an insufficient volume of the remaining liver for radical first-stage resection. The generally accepted safe minimum FLR (future liver remnant) threshold for hepatectomy in patients varies as 20% for a normal liver, 30% for a chemotherapy-related injured liver, and 40% for a cirrhotic liver (Abdalla, Adam et al. 2006, Ribero, Chun et al. 2008). Thus, ensuring adequate FLR is one of the key factors in determining liver tumour resection; the main methods currently used to increase FLR volume include associated liver partition and

portal vein ligation for staged hepatectomy (ALPPS) and portal vein embolization (PVE).

The PVE technique uses percutaneous puncture to apply a steel coil or embolic agent to embolize the affected portal vein and induce hyperplasia in healthy liver tissue; normally, it needs about four to six weeks to achieve sufficient FLR, while ALPPS allows the healthy liver to receive adequate portal venous blood flow and nutrients by blocking the portal trunk of the affected liver and the traffic branches of the healthy liver origin. Comparatively, the short interval between ALLPS procedures (about one to two weeks after surgery) minimises the risk of tumour progression and results in a higher tumour resection rate than PVE, but PVE is less invasive (Schadde, Ardiles et al. 2014, Lau, Lai et al. 2017).

Therefore, for primary hepatocellular carcinoma patients with insufficient FLR, appropriate methods to increase FLR volume should be selected in consideration of the patient's age, tumour and organ function. For example, one study recommended that ALPPS be reserved for FLR/ESLV (estimated standard liver volume) <30% and PVE for FLR/ESLV 30% to 40% (Chan, Zhang et al. 2021).

To evaluate post-hepatectomy liver regeneration in patients, many studies on the predictors of liver regeneration have also been conducted during PVE or ALPPS procedure. For example, Sparrelid et al. sampled plasma at six time points and collected liver lobe biopsies at both stages of ALPPS from 10 patients with colorectal liver metastases treated with neoadjuvant chemotherapy and ALPPS. They measured the levels of several mediators such as IL-6, HGF (hepatocyte growth factor), TNF-α, EGF (epidermal growth factor), and VEGF (vascular endothelial growth factor) in plasma at each time point and detected the expression of mRNA for markers of proliferation and apoptosis in biopsies from the left and right lobes taken at both stages. Through regression analysis, they found that IL-6 and HGF seem to be early mediators of hypertrophy after stage 1 of the ALPPS procedure. Moreover, the peak HGF plasma

level correlated with the degree of FLR growth in patients subjected to ALPPS (Sparrelid, Johansson et al. 2018).

Similarly, Hoekstra et al. also found that serum bile salts and TG (triglyceride) at 5 h after PVE positively correlated with an increase in FLR volume. Following liver surgery, serum TG levels at 5 h and 1 day after resection were associated with liver remnant volume after three months (Hoekstra, van Lienden et al. 2012). Hayashi et al. further confirmed that the increase of the serum bile acid level in patients on day 3 after PVE is a useful predictor of effective hypertrophy of the non-embolized lobe (Hayashi, Beppu et al. 2009).

Therefore, we queried whether the lipid metabolism enzymes involved in our study are correlated with liver regeneration in patients following surgery. Accordingly, we selected three patients who underwent treatment ALPPS to achieve sufficient FLR before liver resection. Consistent with above studies, we extracted small pieces of the hypotrophy and the hypertrophy of liver tissue directly and compared the expression of SCD1 respectively.

In combination with the assessment of liver regeneration volumetry after ALPPS intervention in three patients, as we hypothesised, we found that the expression of SCD1 was higher in the patient who had the highest regeneration index in the liver after intervention. Although there was not a significant difference due to the limited number of cases, it is still a promising tendency and could eventually leads to a new treatment strategy in clinical application. Further studies are indicated, with a larger number of patients.

In conclusion, this antibiotic-treated mouse liver resection model could provide a reference for the rational use of antibiotics in the perioperative period for clinical liver surgery patients if necessary.

6 SUMMARY

In this study, using an experimental antibiotic-treated mouse model, we found that liver regeneration was severely impaired and the survival rate was decreased in antibiotic-treated mice after partial hepatectomy due to the dysbiosis of gut microbiota. Furthermore, compared with control mice, the expression of various cell cycle regulators was also significantly decreased in antibiotic-treated mice at most timepoints after partial hepatectomy. In the end, building on the results of our colleagues, the promoting influence of SCD1 on hepatoma cell proliferation was confirmed by an in vitro assay. Importantly, the relationship between SCD1 and liver regeneration in patients was also investigated.

In summary, our study established a mouse model of partial hepatectomy with antibiotic treatment to investigate the effect of the gut microbiota on liver regeneration. The results revealed that perioperative antibiotic therapy affects the balance of commensal bacteria and could impair liver regeneration. This may lead to a new strategy regarding the use of antibiotics in patients around the time of liver surgery. Furthermore, we also found that SCD1 could be a predictor of liver regeneration in patients.

7 ABBREVIATIONS

ALPPS	Associating liver partition and portal vein ligation for staged hepatectomy
AMPK	AMP-activated protein kinase
BAs	Bile acids
CT	Computed Tomography
E2f	E2 factor
EGF	Epidermal growth factor
ELOVL6	Elongation of very long chain fatty acids protein 6
ESLV	Estimated standard liver volume
FASN	Fatty acid synthase
FLR	Future liver remnant
GC-MS/MS	Gas Chromatography-Tandem Mass Spectrometry
HCC	Hepatocellular carcinoma
HGF	Hepatocyte growth factor
Hippo/YAP	Hippo/Yes-associated protein
IgA	Immunoglobulin A
IHC	Immunohistochemistry
IL-6	Interleukin-6
LPS	Lipopolysaccharides
LR	Liver regeneration
MAMPs	Microbial-associated molecular patterns

MTT	3-(4,5-dimethylthiazol-2-yl)-2,5-diphenyltetrazolium bromide
PC	Phosphatidylcholine
PDK1	Phosphoinositide-dependent kinase-1
PHx	Partial hepatectomy
PPARs	Peroxisome proliferator-activated receptors
PTEN	Phosphatase and tensin homolog
PVE	Portal vein embolization
SCFAs	Short-chain fatty acids
SCD1	Stearoyl-CoA desaturase1
TG	Triglyceride
TGF-β	Transforming growth factor beta
TMA	Trimethylamine
TMAO	Trimethylamine N-oxide
TNF-α	Tumour necrosis factor alpha
TLR4	Toll-like receptors 4
VEGF	Vascular endothelial growth factor
VLDL	Very low-density lipoprotein

8 LIST OF FIGURES

9 REFERENCES

Cullen, J. M. and M. J. Stalker (2016). "Liver and Biliary System." Jubb, Kennedy & Palmer's Pathology of Domestic Animals: Volume 2: 258-352.e251.

Chamberlain, R. S. (2003). Hepatobiliary surgery, CRC Press.

Eipel, C., K. Abshagen and B. Vollmar (2010). "Regulation of hepatic blood flow: the hepatic arterial buffer response revisited." World journal of gastroenterology: WJG **16**(48): 6046.

Strazzabosco, M. and L. Fabris (2008). "Functional anatomy of normal bile ducts." Anatomical record (Hoboken, N.J. : 2007) **291**(6): 653-660.

Michalopoulos, G. K. and M. C. DeFrances (1997). "Liver regeneration." Science **276**(5309): 60-66.

Tao, Y., M. Wang, E. Chen and H. Tang (2017). "Liver Regeneration: Analysis of the Main Relevant Signaling Molecules." Mediators Inflamm **2017**: 4256352.

Sender, R., S. Fuchs and R. Milo (2016). "Revised Estimates for the Number of Human and Bacteria Cells in the Body." PLoS Biol **14**(8): e1002533.

Natividad, J. M. and E. F. Verdu (2013). "Modulation of intestinal barrier by intestinal microbiota: pathological and therapeutic implications." Pharmacol Res **69**(1): 42-51.

den Besten, G., K. van Eunen, A. K. Groen, K. Venema, D. J. Reijngoud and B. M. Bakker (2013). "The role of short-chain fatty acids in the interplay between diet, gut microbiota, and host energy metabolism." J Lipid Res **54**(9): 2325-2340.

Baumler, A. J. and V. Sperandio (2016). "Interactions between the microbiota and pathogenic bacteria in the gut." Nature **535**(7610): 85-93.

Gensollen, T., S. S. Iyer, D. L. Kasper and R. S. Blumberg (2016). "How colonization

by microbiota in early life shapes the immune system." Science **352**(6285): 539-544.

Routy, B., E. Le Chatelier, L. Derosa, C. P. Duong, M. T. Alou, R. Daillère, A. Fluckiger, M. Messaoudene, C. Rauber and M. P. Roberti (2018). "Gut microbiome influences efficacy of PD-1–based immunotherapy against epithelial tumors." Science **359**(6371): 91-97.

Matson, V., J. Fessler, R. Bao, T. Chongsuwat, Y. Zha, M. L. Alegre, J. J. Luke and T. F. Gajewski (2018). "The commensal microbiome is associated with anti-PD-1 efficacy in metastatic melanoma patients." Science **359**(6371): 104-108.

Alexander, C., K. S. Swanson, G. C. Fahey and K. A. Garleb (2019). "Perspective: Physiologic Importance of Short-Chain Fatty Acids from Nondigestible Carbohydrate Fermentation." Adv Nutr **10**(4): 576-589.

den Besten, G., K. Lange, R. Havinga, T. H. van Dijk, A. Gerding, K. van Eunen, M. Muller, A. K. Groen, G. J. Hooiveld, B. M. Bakker and D. J. Reijngoud (2013). "Gut-derived short-chain fatty acids are vividly assimilated into host carbohydrates and lipids." Am J Physiol Gastrointest Liver Physiol **305**(12): G900-910.

Tripathi, A., J. Debelius, D. A. Brenner, M. Karin, R. Loomba, B. Schnabl and R. Knight (2018). "The gut-liver axis and the intersection with the microbiome." Nat Rev Gastroenterol Hepatol **15**(7): 397-411.

Higgins, G. M. (1931). "Experimental pathology of the liver. Restoration of the liver of the white rat following partial surgical removal." AMA Arch Pathol **12**: 186-202.

Yokoyama, H. O., M. E. Wilson, K. K. Tsuboi and R. E. Stowell (1953). "Regeneration of mouse liver after partial hepatectomy." Cancer research **13**(1): 80-85.

Mitchell, C. and H. Willenbring (2008). "A reproducible and well-tolerated method for 2/3 partial hepatectomy in mice." Nat Protoc **3**(7): 1167-1170.

Lamouse-Smith, E. S., A. Tzeng and M. N. Starnbach (2011). "The intestinal flora is required to support antibody responses to systemic immunization in infant and germ free mice." PLoS One **6**(11): e27662.

Deshmukh, H. S., Y. Liu, O. R. Menkiti, J. Mei, N. Dai, C. E. O'Leary, P. M. Oliver, J. K. Kolls, J. N. Weiser and G. S. Worthen (2014). "The microbiota regulates neutrophil homeostasis and host resistance to Escherichia coli K1 sepsis in neonatal mice." Nat Med **20**(5): 524-530.

Gonzalez-Perez, G., A. L. Hicks, T. M. Tekieli, C. M. Radens, B. L. Williams and E. S. Lamouse-Smith (2016). "Maternal Antibiotic Treatment Impacts Development of the Neonatal Intestinal Microbiome and Antiviral Immunity." J Immunol **196**(9): 3768-3779.

Li, F., X. Hao, Y. Chen, L. Bai, X. Gao, Z. Lian, H. Wei, R. Sun and Z. Tian (2017). "The microbiota maintain homeostasis of liver-resident gammadeltaT-17 cells in a lipid antigen/CD1d-dependent manner." Nat Commun **7**: 13839.

Atarashi, K., T. Tanoue, T. Shima, A. Imaoka, T. Kuwahara, Y. Momose, G. Cheng, S. Yamasaki, T. Saito, Y. Ohba, T. Taniguchi, K. Takeda, S. Hori, Ivanov, II, Y. Umesaki, K. Itoh and K. Honda (2011). "Induction of colonic regulatory T cells by indigenous Clostridium species." Science **331**(6015): 337-341.

Schubert, A. M., H. Sinani and P. D. Schloss (2015). "Antibiotic-Induced Alterations of the Murine Gut Microbiota and Subsequent Effects on Colonization Resistance against Clostridium difficile." mBio **6**(4): e00974.

Abt, M. C., L. C. Osborne, L. A. Monticelli, T. A. Doering, T. Alenghat, G. F. Sonnenberg, M. A. Paley, M. Antenus, K. L. Williams, J. Erikson, E. J. Wherry and D. Artis (2012). "Commensal bacteria calibrate the activation threshold of innate antiviral immunity." Immunity **37**(1): 158-170.

Emal, D., E. Rampanelli, I. Stroo, L. M. Butter, G. J. Teske, N. Claessen, G. Stokman, S. Florquin, J. C. Leemans and M. C. Dessing (2017). "Depletion of Gut Microbiota Protects against Renal Ischemia-Reperfusion Injury." J Am Soc Nephrol **28**(5): 1450-1461.

Tsuei, J., T. Chau, D. Mills and Y. J. Wan (2014). "Bile acid dysregulation, gut dysbiosis, and gastrointestinal cancer." Exp Biol Med (Maywood) **239**(11): 1489-1504.

Liu, H. X., R. Keane, L. Sheng and Y. J. Wan (2015). "Implications of microbiota and bile acid in liver injury and regeneration." J Hepatol **63**(6): 1502-1510.

Rakoff-Nahoum, S., J. Paglino, F. Eslami-Varzaneh, S. Edberg and R. Medzhitov (2004). "Recognition of commensal microflora by toll-like receptors is required for intestinal homeostasis." Cell **118**(2): 229-241.

Martin, F. P., M. E. Dumas, Y. Wang, C. Legido-Quigley, I. K. Yap, H. Tang, S. Zirah, G. M. Murphy, O. Cloarec, J. C. Lindon, N. Sprenger, L. B. Fay, S. Kochhar, P. van Bladeren, E. Holmes and J. K. Nicholson (2007). "A top-down systems biology view of microbiome-mammalian metabolic interactions in a mouse model." Mol Syst Biol **3**: 112.

Larsen, N., F. K. Vogensen, F. W. van den Berg, D. S. Nielsen, A. S. Andreasen, B. K. Pedersen, W. A. Al-Soud, S. J. Sorensen, L. H. Hansen and M. Jakobsen (2010). "Gut microbiota in human adults with type 2 diabetes differs from non-diabetic adults." PLoS One **5**(2): e9085.

Bäckhed, F., H. Ding, T. Wang, L. V. Hooper, G. Y. Koh, A. Nagy, C. F. Semenkovich and J. I. Gordon (2004). "The gut microbiota as an environmental factor that regulates fat storage." Proceedings of the national academy of sciences **101**(44): 15718-15723.

Ley, R. E., F. Bäckhed, P. Turnbaugh, C. A. Lozupone, R. D. Knight and J. I. Gordon (2005). "Obesity alters gut microbial ecology." Proceedings of the national academy of

sciences **102**(31): 11070-11075.

Ley, R. E., P. J. Turnbaugh, S. Klein and J. I. Gordon (2006). "Human gut microbes associated with obesity." nature **444**(7122): 1022-1023.

Moschen, A. R., S. Kaser and H. Tilg (2013). "Non-alcoholic steatohepatitis: a microbiota-driven disease." Trends Endocrinol Metab **24**(11): 537-545.

Michalik, L., J. Auwerx, J. P. Berger, V. K. Chatterjee, C. K. Glass, F. J. Gonzalez, P. A. Grimaldi, T. Kadowaki, M. A. Lazar, S. O'Rahilly, C. N. Palmer, J. Plutzky, J. K. Reddy, B. M. Spiegelman, B. Staels and W. Wahli (2006). "International Union of Pharmacology. LXI. Peroxisome proliferator-activated receptors." Pharmacol Rev **58**(4): 726-741.

Berger, J. and D. E. Moller (2002). "The mechanisms of action of PPARs." Annual review of medicine **53**(1): 409-435.

Feige, J. N., L. Gelman, L. Michalik, B. Desvergne and W. Wahli (2006). "From molecular action to physiological outputs: peroxisome proliferator-activated receptors are nuclear receptors at the crossroads of key cellular functions." Prog Lipid Res **45**(2): 120-159.

Belfiore, A., M. Genua and R. Malaguarnera (2009). "PPAR-gamma agonists and their effects on IGF-I receptor signaling: Implications for cancer." PPAR Res **2009**: 830501.

Dunning, K. R., M. R. Anastasi, V. J. Zhang, D. L. Russell and R. L. Robker (2014). "Regulation of fatty acid oxidation in mouse cumulus-oocyte complexes during maturation and modulation by PPAR agonists." PLoS One **9**(2): e87327.

Wang, Y. X. (2010). "PPARs: diverse regulators in energy metabolism and metabolic diseases." Cell Res **20**(2): 124-137.

Grygiel-Górniak, B. (2014). "Peroxisome proliferator-activated receptors and their

ligands: nutritional and clinical implications-a review." <u>Nutrition journal</u> **13**(1): 1-10.

Liu, H. X., Y. Fang, Y. Hu, F. J. Gonzalez, J. Fang and Y. J. Wan (2013). "PPARbeta Regulates Liver Regeneration by Modulating Akt and E2f Signaling." <u>PLoS One</u> **8**(6): e65644.

Gazit, V., J. Huang, A. Weymann and D. A. Rudnick (2012). "Analysis of the role of hepatic PPARgamma expression during mouse liver regeneration." <u>Hepatology</u> **56**(4): 1489-1498.

Huang, W., K. Ma, J. Zhang, M. Qatanani, J. Cuvillier, J. Liu, B. Dong, X. Huang and D. D. Moore (2006). "Nuclear receptor-dependent bile acid signaling is required for normal liver regeneration." <u>Science</u> **312**(5771): 233-236.

Bruno, S. and Z. Darzynkiewicz (1992). "Cell cycle dependent expression and stability of the nuclear protein detected by Ki‐67 antibody in HL‐60 cells." <u>Cell proliferation</u> **25**(1): 31-40.

Cornell, R. P. (1985). "Restriction of gut-derived endotoxin impairs DNA synthesis for liver regeneration." <u>American Journal of Physiology-Regulatory, Integrative and Comparative Physiology</u> **249**(5): R563-R569.

Cornell, R. P., B. L. Liljequist and K. F. Bartizal (1990). "Depressed liver regeneration after partial hepatectomy of germ‐free, athymic and lipopolysaccharide‐resistant mice." <u>Hepatology</u> **11**(6): 916-922.

Mosmann, T. (1983). "Rapid colorimetric assay for cellular growth and survival: application to proliferation and cytotoxicity assays." <u>Journal of immunological methods</u> **65**(1-2): 55-63.

Vistica, D. T., P. Skehan, D. Scudiero, A. Monks, A. Pittman and M. R. Boyd (1991). "Tetrazolium-based assays for cellular viability: a critical examination of selected

parameters affecting formazan production." Cancer research **51**(10): 2515-2520.

Popescu, G. A., S. T. Alexandrescu, R. T. Grigorie, L. Stoica, C. A. Apavaloaie and D. Hrehoret (2017). "GOOD TO KNOW: The ALPPS Procedure - Embracing a New Technique." Chirurgia (Bucur) **112**(3): 332-341.

Hirokawa, F., M. Hayashi, Y. Miyamoto, M. Asakuma, T. Shimizu, K. Komeda, Y. Inoue, K. Uchiyama and Y. Nishimura (2013). "Evaluation of postoperative antibiotic prophylaxis after liver resection: a randomized controlled trial." The American Journal of Surgery **206**(1): 8-15.

Parker, G. A. and C. A. Picut (2005). "Liver immunobiology." Toxicol Pathol **33**(1): 52-62.

Racanelli, V. and B. Rehermann (2006). "The liver as an immunological organ." Hepatology **43**(2 Suppl 1): S54-62.

Robinson, M. W., C. Harmon and C. O'Farrelly (2016). "Liver immunology and its role in inflammation and homeostasis." Cell Mol Immunol **13**(3): 267-276.

De La Cochetiere, M. F., T. Durand, P. Lepage, A. Bourreille, J. P. Galmiche and J. Dore (2005). "Resilience of the dominant human fecal microbiota upon short-course antibiotic challenge." J Clin Microbiol **43**(11): 5588-5592.

Puhl, N. J., R. R. Uwiera, L. J. Yanke, L. B. Selinger and G. D. Inglis (2012). "Antibiotics conspicuously affect community profiles and richness, but not the density of bacterial cells associated with mucosa in the large and small intestines of mice." Anaerobe **18**(1): 67-75.

Panda, S., I. El khader, F. Casellas, J. Lopez Vivancos, M. Garcia Cors, A. Santiago, S. Cuenca, F. Guarner and C. Manichanh (2014). "Short-term effect of antibiotics on human gut microbiota." PLoS One **9**(4): e95476.

Wu, X., R. Sun, Y. Chen, X. Zheng, L. Bai, Z. Lian, H. Wei and Z. Tian (2015). "Oral ampicillin inhibits liver regeneration by breaking hepatic innate immune tolerance normally maintained by gut commensal bacteria." Hepatology **62**(1): 253-264.

Eyssen, H. and G. Parmentier (1974). "Biohydrogenation of sterols and fatty acids by the intestinal microflora." Am J Clin Nutr **27**(11): 1329-1340.

Hedrich, H. (2004). The laboratory mouse, Academic Press.

Voravuthikunchai, S. P. and A. Lee (1987). "Cecectomy causes long-term reduction of colonization resistance in the mouse gastrointestinal tract." Infection and immunity **55**(4): 995-999.

Blaut, M. and T. Clavel (2007). "Metabolic diversity of the intestinal microbiota: implications for health and disease." The Journal of nutrition **137**(3): 751S-755S.

Louis, P. and H. J. Flint (2009). "Diversity, metabolism and microbial ecology of butyrate-producing bacteria from the human large intestine." FEMS Microbiol Lett **294**(1): 1-8.

Louis, P., P. Young, G. Holtrop and H. J. Flint (2010). "Diversity of human colonic butyrate-producing bacteria revealed by analysis of the butyryl-CoA:acetate CoA-transferase gene." Environ Microbiol **12**(2): 304-314.

Levy, M., C. A. Thaiss and E. Elinav (2016). "Metabolites: messengers between the microbiota and the immune system." Genes & development **30**(14): 1589-1597.

Feng, W., H. Ao and C. Peng (2018). "Gut Microbiota, Short-Chain Fatty Acids, and Herbal Medicines." Front Pharmacol **9**: 1354.

Cummings, J., E. Pomare, W. Branch, C. Naylor and G. MacFarlane (1987). "Short chain fatty acids in human large intestine, portal, hepatic and venous blood." Gut **28**(10): 1221-1227.

Al-Lahham, S. H., M. P. Peppelenbosch, H. Roelofsen, R. J. Vonk and K. Venema (2010). "Biological effects of propionic acid in humans; metabolism, potential applications and underlying mechanisms." Biochim Biophys Acta **1801**(11): 1175-1183.

Delzenne, N. M. and C. M. Williams (2002). "Prebiotics and lipid metabolism." Current opinion in lipidology **13**(1): 61-67.

De Vadder, F., P. Kovatcheva-Datchary, D. Goncalves, J. Vinera, C. Zitoun, A. Duchampt, F. Bäckhed and G. Mithieux (2014). "Microbiota-Generated Metabolites Promote Metabolic Benefits via Gut-Brain Neural Circuits." Cell **156**(1-2): 84-96.

Sakata, T. and W. Von Engelhardt (1983). "Stimulatory effect of short chain fatty acids on the epithelial cell proliferation in rat large intestine." Comparative biochemistry and physiology. A, Comparative physiology **74**(2): 459-462.

Ichikawa, H., R. Shineha, S. Satomi and T. Sakata (2002). "Gastric or rectal instillation of short-chain fatty acids stimulates epithelial cell proliferation of small and large intestine in rats." Digestive diseases and sciences **47**(5): 1141-1146.

Esko, J. D. and C. Raetz (1980). "Autoradiographic detection of animal cell membrane mutants altered in phosphatidylcholine synthesis." Proceedings of the National Academy of Sciences **77**(9): 5192-5196.

Sharma, V. K., S. K. Ghosh, P. Mandal, T. Yamada, K. Shibata, S. Mitra and R. Mukhopadhyay (2017). "Effects of ionic liquids on the nanoscopic dynamics and phase behaviour of a phosphatidylcholine membrane." Soft Matter **13**(47): 8969-8979.

Tzur, A., R. Kafri, V. S. LeBleu, G. Lahav and M. W. Kirschner (2009). "Cell growth and size homeostasis in proliferating animal cells." Science **325**(5937): 167-171.

McCusker, D. and D. R. Kellogg (2012). "Plasma membrane growth during the cell cycle: unsolved mysteries and recent progress." Curr Opin Cell Biol **24**(6): 845-851.

Alberts, B., A. Johnson, J. Lewis, P. Walter, M. Raff and K. Roberts (2002). Molecular Biology of the Cell 4th Edition: International Student Edition, Routledge.

Kidd, P. M. (1996). "Phosphatidylcholine, a superior protectant against liver damage." Altern Med Rev **1**(4): 258-274.

Guillou, H., D. Zadravec, P. G. Martin and A. Jacobsson (2010). "The key roles of elongases and desaturases in mammalian fatty acid metabolism: Insights from transgenic mice." Prog Lipid Res **49**(2): 186-199.

Ran, H., Y. Zhu, R. Deng, Q. Zhang, X. Liu, M. Feng, J. Zhong, S. Lin, X. Tong and Q. Su (2018). "Stearoyl-CoA desaturase-1 promotes colorectal cancer metastasis in response to glucose by suppressing PTEN." J Exp Clin Cancer Res **37**(1): 54.

Gao, Y., J. Li, H. Xi, J. Cui, K. Zhang, J. Zhang, Y. Zhang, W. Xu, W. Liang, Z. Zhuang, P. Wang, Z. Qiao, B. Wei and L. Chen (2020). "Stearoyl-CoA-desaturase-1 regulates gastric cancer stem-like properties and promotes tumour metastasis via Hippo/YAP pathway." Br J Cancer **122**(12): 1837-1847.

Huang, G. M., Q. H. Jiang, C. Cai, M. Qu and W. Shen (2015). "SCD1 negatively regulates autophagy-induced cell death in human hepatocellular carcinoma through inactivation of the AMPK signaling pathway." Cancer Lett **358**(2): 180-190.

Abdalla, E. K., R. Adam, A. J. Bilchik, D. Jaeck, J.-N. Vauthey and D. Mahvi (2006). "Improving Resectability of Hepatic Colorectal Metastases: Expert Consensus Statement." Annals of Surgical Oncology **13**(10): 1271-1280.

Ribero, D., Y. S. Chun and J. N. Vauthey (2008). "Standardized liver volumetry for portal vein embolization." Semin Intervent Radiol **25**(2): 104-109.

Schadde, E., V. Ardiles, K. Slankamenac, C. Tschuor, G. Sergeant, N. Amacker, J. Baumgart, K. Croome, R. Hernandez-Alejandro, H. Lang, E. de Santibanes and P. A.

Clavien (2014). "ALPPS offers a better chance of complete resection in patients with primarily unresectable liver tumors compared with conventional-staged hepatectomies: results of a multicenter analysis." World J Surg **38**(6): 1510-1519.

Lau, W. Y., E. C. H. Lai and S. H. Y. Lau (2017). "Associating liver partition and portal vein ligation for staged hepatectomy: the current role and development." Hepatobiliary & Pancreatic Diseases International **16**(1): 17-26.

Chan, A., W. Y. Zhang, K. Chok, J. Dai, R. Ji, C. Kwan, N. Man, R. Poon and C. M. Lo (2021). "ALPPS Versus Portal Vein Embolization for Hepatitis-related Hepatocellular Carcinoma: A Changing Paradigm in Modulation of Future Liver Remnant Before Major Hepatectomy." Ann Surg **273**(5): 957-965.

Sparrelid, E., H. Johansson, S. Gilg, G. Nowak, E. Ellis and B. Isaksson (2018). "Serial Assessment of Growth Factors Associated with Liver Regeneration in Patients Operated with Associating Liver Partition and Portal Vein Ligation for Staged Hepatectomy." Eur Surg Res **59**(1-2): 72-82.

Hoekstra, L. T., K. P. van Lienden, F. G. Schaap, R. A. Chamuleau, R. J. Bennink and T. M. van Gulik (2012). "Can plasma bile salt, triglycerides, and apoA-V levels predict liver regeneration?" World J Surg **36**(12): 2901-2908.

Hayashi, H., T. Beppu, H. Sugita, K. Horino, H. Komori, T. Masuda, H. Okabe, H. Takamori and H. Baba (2009). "Increase in the serum bile acid level predicts the effective hypertrophy of the nonembolized hepatic lobe after right portal vein embolization." World J Surg **33**(9): 1933-1940.

10 CURRICULUM VITAE

Name: Yuhan Yin

Date of birth: 07/10/1992

Place of birth: Liaoning, China

Nationality: Chinese

E-mail: yuhanyin1007@126.com / yuhan.yin@tum.de

University Education:

09.2011-06.2016, Bachelor's degree of medicine, School of Clinical Medicine, Zhengzhou University, Zhengzhou, China

09.2016-06.2018, Master's degree of medicine, Graduate School of Clinical Medicine, Zhengzhou University, Zhengzhou, China

10.2018 until now, medical doctoral candidate, TUM Medical Graduate Centre, Technical University of Munich

Publications:

Zhang, X. J., V. Olsavszky, **Y. Yin**, B. Wang, T. Engleitner, R. Ollinger, K. Schledzewski, P. S. Koch, R. Rad, R. M. Schmid, H. Friess, S. Goerdt, N. Huser, C. Geraud, G. von Figura and D. Hartmann (2020). "Angiocrine Hepatocyte Growth Factor Signaling Controls Physiological Organ and Body Size and Dynamic Hepatocyte Proliferation to Prevent Liver Damage during Regeneration." Am J Pathol 190(2): 358-371.

Fu, Y., G. Yang, P. Xue, L. Guo, **Y. Yin**, Z. Ye, S. Peng, Y. Qin, Q. Duan and F. Zhu (2018). "Dasatinib reduces 5-Fu-triggered apoptosis in colon carcinoma by directly modulating Src-dependent caspase-9 phosphorylation." Cell death discovery 4(1): 1-8.

The thesis related manuscript was submitted to the "*Journal of Hepatology*" and under revision at the time of thesis submission.

Parts of this thesis was presented at the following scientific conferences:

1. Scientific e-poster presentation.

Title: Influence of the gut microbiome on liver regeneration

Conference name: UEG Week Virtual 2020

Conference organizer: United European Gastroenterology

Conference date:11.10.2020 – 13.10.2020

Conference place: In virtual

2. Scientific e-poster presentation.

Title: The influence of intestinal flora on liver regeneration through the liver-gut axis

Conference name: Online Live Event 'Liver-Gut-Axis'

Conference organizer: Falk Foundation e.V.

Conference date: 28.01.2021 - 29.01.2021

Conference place: In Virtual

11 ACKNOWLEDGEMENTS